Cell Reports
Medicine

Article

Th2-like T Follicular Helper Cells Promote Functional Antibody Production during *Plasmodium falciparum* Infection

Graphical Abstract

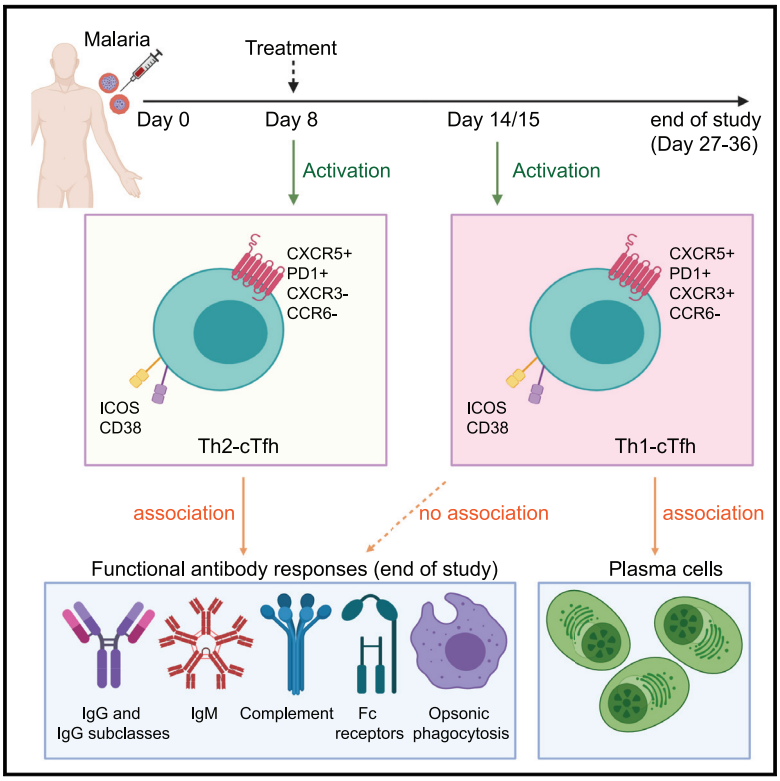

Highlights

- T follicular helper (Tfh) cells are activated following experimental malaria infection
- Th2-Tfh cells activate at peak infection, and Th1-Tfh cells activate after treatment
- Functional anti-malarial antibodies are induced following experimental infection
- Functional antibodies associate with Th2-Tfh cell activation during peak infection

Authors

Jo-Anne Chan, Jessica R. Loughland, Fabian de Labastida Rivera, ..., James G. Beeson, Christian R. Engwerda, Michelle J. Boyle

Correspondence

michelle.boyle@qimrberghofer.edu.au

In Brief

Chan et al. used experimental *P. falciparum* malaria infection in Australian adults to study Tfh cell activation and antibody induction. They provide evidence for an association between Th2-Tfh activation and induction of functional antibodies against malaria. Data inform the development of malaria vaccines targeting Th2-Tfh cells to boost antibody induction.

Chan et al., 2020, Cell Reports Medicine *1*, 100157
December 22, 2020
https://doi.org/10.1016/j.xcrm.2020.100157

CellPress

Cell Reports Medicine

CellPress
OPEN ACCESS

Article

Th2-like T Follicular Helper Cells Promote Functional Antibody Production during *Plasmodium falciparum* Infection

Jo-Anne Chan,[1,2,4] Jessica R. Loughland,[6] Fabian de Labastida Rivera,[6] Arya SheelaNair,[6] Dean W. Andrew,[6] Nicholas L. Dooley,[6] Bruce D. Wines,[1,2,5] Fiona H. Amante,[6] Lachlan Webb,[6] P. Mark Hogarth,[1,2,5] James S. McCarthy,[6] James G. Beeson,[1,3,4] Christian R. Engwerda,[6] and Michelle J. Boyle[1,6,7,*]

[1]Life Sciences, Burnet Institute, Melbourne, VIC 3004, Australia
[2]Department of Immunology, Central Clinical School, Monash University, Melbourne, VIC 3004, Australia
[3]Department of Microbiology, Central Clinical School, Monash University, Melbourne, VIC 3004, Australia
[4]Department of Medicine, University of Melbourne, Parkville, VIC 3052, Australia
[5]Department of Clinical Pathology, University of Melbourne, Parkville, VIC 3052, Australia
[6]QIMR-Berghofer Medical Research Institute, Herston, QLD 4006, Australia
[7]Lead Contact
*Correspondence: michelle.boyle@qimrberghofer.edu.au
https://doi.org/10.1016/j.xcrm.2020.100157

SUMMARY

CD4$^+$ T follicular helper cells (Tfh) are key drivers of antibody development. During *Plasmodium falciparum* malaria in children, the activation of Tfh is restricted to the Th1 subset and not associated with antibody levels. To identify Tfh subsets that are associated with antibody development in malaria, we assess Tfh and antibodies longitudinally in human volunteers with experimental *P. falciparum* infection. Tfh cells activate during infection, with distinct dynamics in different Tfh subsets. Th2-Tfh cells activate early, during peak infection, while Th1-Tfh cells activate 1 week after peak infection and treatment. Th2-Tfh cell activation is associated with the functional breadth and magnitude of parasite antibodies. In contrast, Th1-Tfh activation is not associated with antibody development but instead with plasma cells, which have previously been shown to play a detrimental role in the development of long-lived immunity. Thus, our study identifies the contrasting roles of Th2 and Th1-Tfh cells during experimental *P. falciparum* malaria.

INTRODUCTION

Malaria caused by *Plasmodium falciparum* remains one of the most important infectious diseases globally, with >200 million clinical cases and up to 500,000 deaths annually.[1] Antibodies play a major role in naturally acquired and vaccine-induced protective immunity to malaria, but factors that determine their optimal induction and maintenance over time are poorly understood. The first licensed malaria vaccine, RTS,S, prevents infection by inducing antibodies that target sporozoites,[2–4] and large-scale Phase IV implementation trials of RTS,S have recently commenced in parts of Africa. Despite this, RTS,S has only moderate efficacy and short-lived protection in the target population of infants and young children.[4] Thus, understanding the induction and maintenance of protective antibodies is crucial for developing vaccines with greater efficacy and durability.

Antibody production, both during infection and vaccination, is driven by CD4$^+$ T follicular helper (Tfh) cells, which promote the development of memory and class-switched, affinity-mature antibody-producing B cells.[5] Due to the central importance of Tfh cells in antibody induction, the optimized targeting of these cells has been proposed as a key avenue to develop improved malaria vaccines.[6,7] Tfh cells primarily function within germinal centers (GCs).[5] However, in humans, subsets of peripheral blood circulating CD4$^+$ T cells, which express CXCR5 and programmed cell death protein 1 (PD1) molecules, share phenotypic, functional, and transcriptional profiles of and significant clonal overlap with lymphoid Tfh cells.[8–11] Upon activation, circulating Tfh (cTfh) cells express the co-stimulatory marker ICOS, which is crucial for development and function,[12–14] as well as other activation markers, including CD38 and Ki67.[15] cTfh can be segregated into 3 different T helper (Th)-like subsets based on CXCR3 and CCR6 expression: Th1 (CXCR3$^+$CCR6$^-$), Th2 (CXCR3$^-$CCR6$^-$), and Th17 (CXCR3$^-$CCR6$^+$).[11] Th2-cTfh cells exhibit transcriptional profiles that are most closely related to GC Tfh cells,[10] and, along with Th17-cTfh cells, have the greatest capacity to activate naive B cells *in vitro*.[11] The relative importance of specific cTfh cell subsets in driving antibody responses appears to be influenced by the type of pathogen and context of the exposure. For example, Th2-cTfh cells have been associated with the acquisition of broadly neutralizing antibodies against HIV,[10] while Th1-cTfh cells are linked to the induction of antibodies following viral infection and vaccination, including influenza, HIV, and severe acute respiratory syndrome-coronavirus-2 (SARS-CoV-2).[16–19]

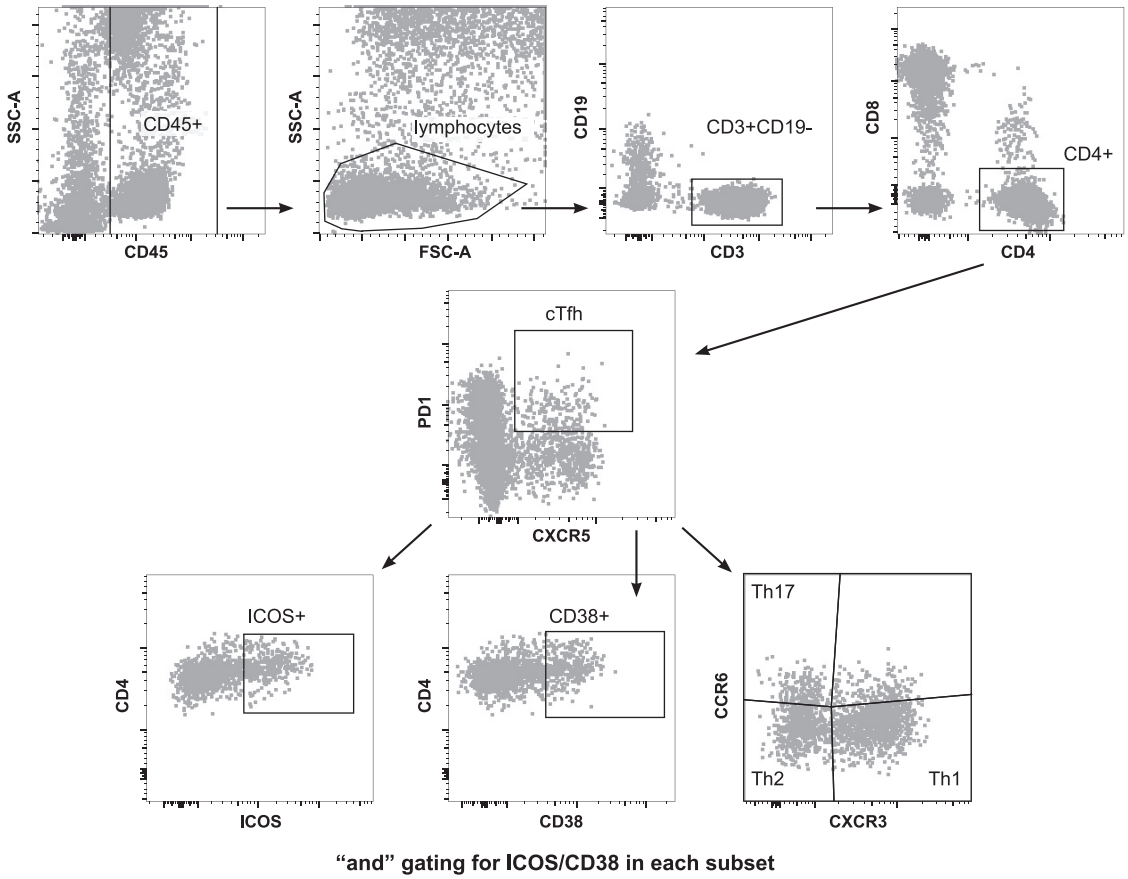

Figure 1. Gating Strategy for Tfh in Whole Blood

Gating strategy to identify cTfH, activation, and subsets. Whole blood was stained and analyzed by flow cytometry, and $CD45^+$ lymphocytes were gated as T cells on CD3. CD4 T cells were gated as $CD4^+CD8^-$ and cTfh analyzed based on $PD1^+CXCR5^+$ cells. cTfh cell subsets were analyzed based on CXCR3 and CCR6 staining into Th1 ($CXCR3^+CCR6^-$), Th17 ($CXC3^-CCR6^+$), and Th2 ($CXCR3^-CCR6^-$). Activation was gated as $ICOS^+$ and $CD38^+$ "and" gates were made to assess activation markers within subsets. Data are representative of 157 samples (40 individuals at days 0, 8, and 14/15 and 37 individuals at EOS).

cTfh cell activation during *P. falciparum* infection in humans has only been investigated in a single study of Malian children.[20] This study reported that during *P. falciparum* malaria, cTfh cell activation was restricted to Th1-cTfh cells, and activation was not correlated with anti-malarial immunoglobulin G (IgG) responses.[20] Th1-cTfh cells have been linked to the development of atypical memory B cells,[21] which have exhausted phenotypes during malaria.[22,23] Furthermore, murine models have shown that Th1-Tfh skewing by malaria-induced inflammation is detrimental to GC formation and antibody induction.[24] These data support the hypothesis that the preferential activation of Th1-Tfh cells during malaria slows the acquisition of protective anti-malarial antibodies.[25] However, protective antibodies to malaria do develop over time in exposed populations, and it remains unknown whether cTfh cell activation plays a role in antibody acquisition and maintenance in humans.

We hypothesized that Th2-cTfh cell activation during *P. falciparum* infection, rather than Th1-cTfH, is required to promote effective anti-malarial antibody production. To test this hypothesis, we experimentally infected malaria-naive Australian adult volunteers using the induced blood stage malaria (IBSM) system. This allowed us to evaluate the immune response induced following a single *P. falciparum* infection, without the influence of prior malaria exposure or other comorbidities observed in endemic populations that can confound the analysis and interpretation of findings.[26] We quantified cTfh cell activation and antibody magnitude, type, and functional activity during experimental *P. falciparum* infection in a group of 40 volunteers and assessed the associations between cTfh and antibody induction. Our results identify cTfh cell subsets and phenotypes that are associated with the induction of functional antibodies required for protection from human malaria infection.

RESULTS

cTfh Cells Upregulate Multiple Activation Markers during IBSM

To assess cTfh cells during malaria infection, we quantified cTfh cell activation and subset distribution by flow cytometry in a large cohort of IBSM participants (n = 40) (Figure 1). The activation of cTfh cells was assessed with the commonly used activation markers ICOS and CD38. While the frequency of cTfh cells among circulating $CD4^+$ T cells remained

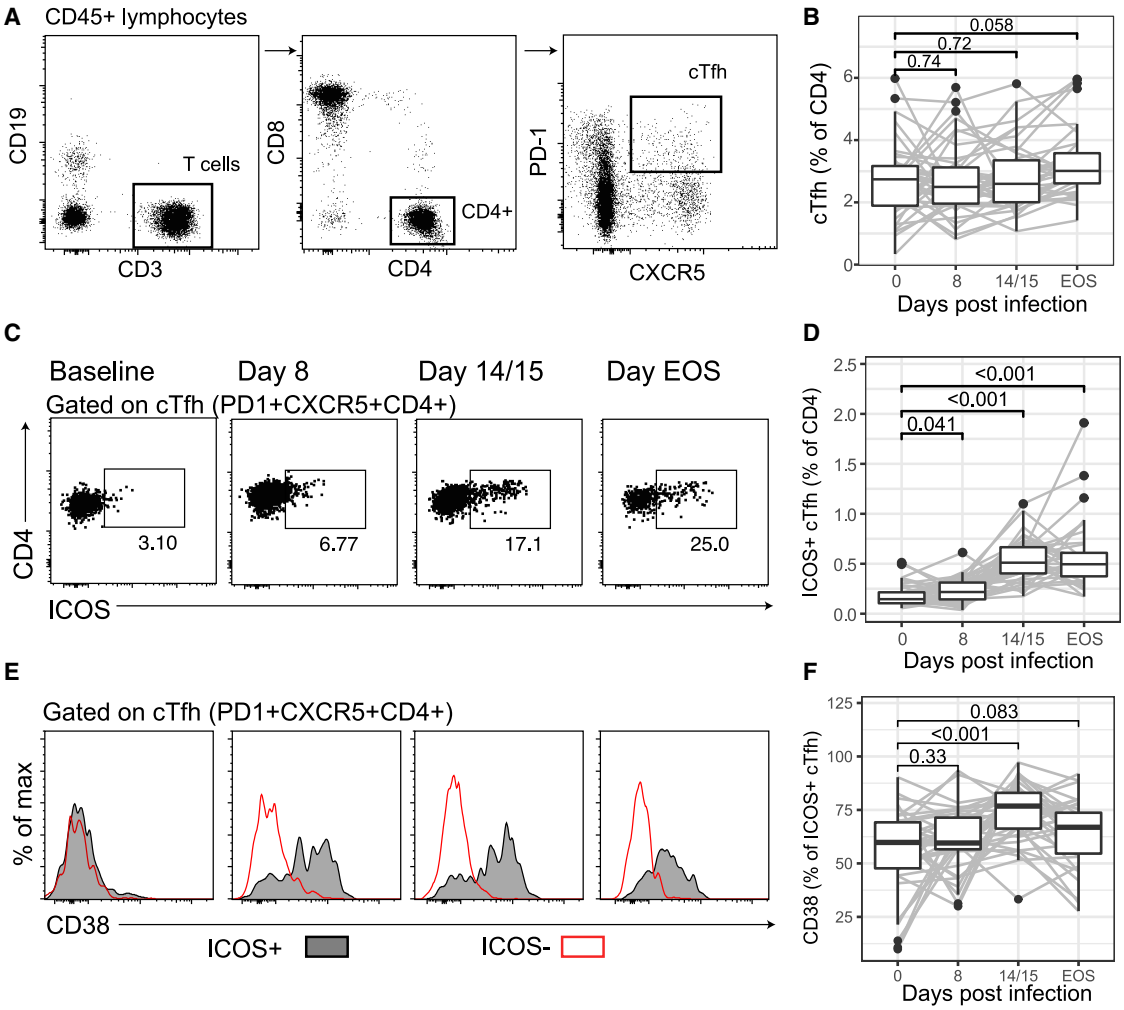

Figure 2. cTfh Are Activated in *P. falciparum* Infection

(A) cTfh ($PD1^+CXCR5^+CD4$) T cells were assessed by flow cytometry at days 0, 8, and 14/15, and EOS.

(B) cTfh cells as a frequency of total CD4 T cells after infection.

(C) Representative flow cytometry gating of activated ($ICOS^+$) cTfh cells following infection.

(D) Activated cTfh ($ICOS^+$) cells as a frequency of CD4 T cells.

(E) Representative histograms of CD38 expression on activated ($ICOS^+$) and non-activated ($ICOS^-$) cTfh cells.

(F) CD38 positivity as a frequency of activated $ICOS^+$ cTfh cells. Flow cytometry-based assays were performed once on whole-blood samples tested in singles. Data are from 40 individuals at days 0, 8, and 14/15 and 37 individuals at EOS. (A), (C), and (E) are representative data from a single individual. For (B), (D), and (F), paired Wilcoxon signed-rank tests compared to day 0 are indicated. Boxplots are Tukey style, with median and interquartile range (IQR). Whiskers are to data point no further than 1.5 × IQR; dots are outlying points. Paired data are joined by lines. See also Figures S1 and S2.

unchanged (Figures 2A and 2B), ICOS was upregulated at peak infection, and further increased by day 14/15 and end of study (EOS) (Figures 2C and 2D). There was no correlation between pre-infection levels of ICOS and the magnitude of upregulation during infection (Figure S1A). Furthermore, ICOS upregulation was not correlated with parasite biomass, which varied substantially among participants (Figures S1B and S1C). $ICOS^+$ cTfh cells but not $ICOS^-$ counterparts also expressed the activation marker CD38, which increased following treatment at day 14/15 (Figures 2E and 2F). Ki67 and human leukocyte antigen-DR isotype (HLA-DR) expression was also evident among cTfh and was higher on $ICOS^+$ compared to $ICOS^-$ cTfh cells indicating that multiple activation markers were increased during infection (Figure S2).

Th2-cTfh Cells Are Activated Early in Infection, whereas Th1-cTfh Cells Are Activated after Drug Treatment

When divided into Th1, Th2, and Th17 subsets based on CXCR3 and CCR6 expression (Figure 1), the proportion of Th2-cTfh cells increased at day 8 (peak infection) compared to pre-infection. However, after drug treatment, the proportion of Th2-cTfh cells returned to baseline, whereas there was a marked increase in the proportion of Th1-cTfh cells (Figure 3A). Similarly, there was an increase in activated $ICOS^+$ and $CD38^+$ Th2-cTfh cells

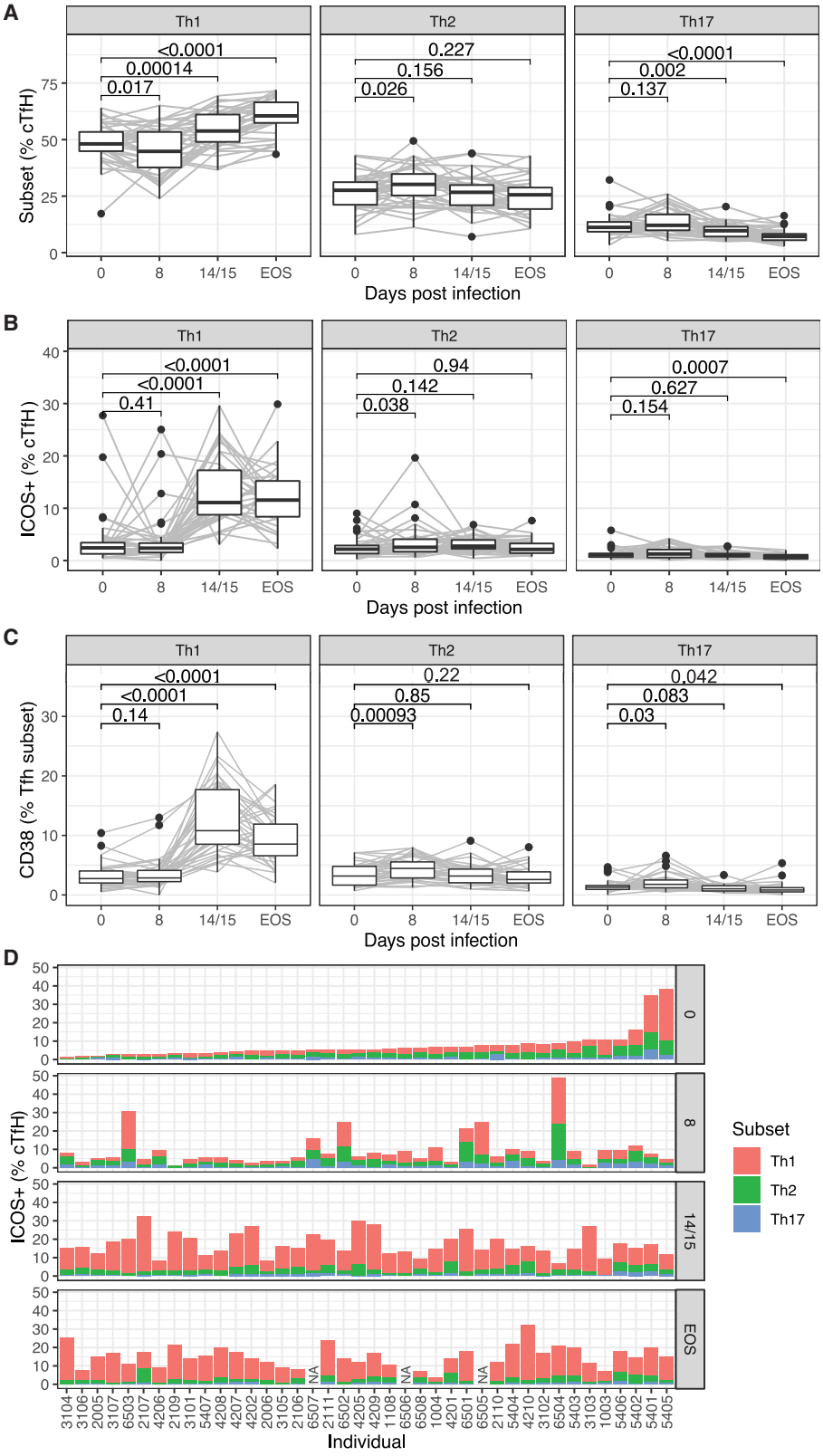

(legend on next page)

but not in Th1-cTfh cells at peak infection (Figures 3B and 3C). $CD38^+$ but not $ICOS^+$ Th17-cTfh cells were also increased at peak infection (Figures 3B and 3C). In contrast, following drug treatment, there was a large increase in $ICOS^+$ and $CD38^+$ Th1-cTfh, but this was not observed for the other subsets (Figures 3B and 3C). While significant changes were detected among the population, it should be noted that there was substantial variation in the subset composition of cTfh cell activation between individuals (Figure 3D). These data indicated that in contrast to reports in Malian children with *P. falciparum* malaria, in which cTfh activation is restricted to Th1-cTfh cells,[20] during experimental *P. falciparum* infection multiple cTfh cell subsets were phenotypically activated, but activation occurs with different kinetics. Our results demonstrate that Th2-cTfh cells were predominantly activated early, during peak infection (day 8 post-infection), while Th1-cTfh cell activation occurred post-treatment (day 14/15 post-infection and EOS), and subsequently dominated the cTfh cell response.

Memory Distribution between Tfh Subsets and Changes following Malaria Infection

To further investigate cTfh phenotypes during infection, subsequent analysis of Tfh during IBSM was performed on a single cohort (n = 6) of participants with available peripheral blood mononuclear cell (PBMC) samples (at days 0, 8, and EOS). The memory phenotype of cTfh cells was assessed by CD45RA and CCR7 and memory phenotypes were classified as central memory (CM, $CD45RA^-CCR7^+$), effector memory (EM, $CD45RA^-CCR7^-$), terminally differentiated effector memory (TEMRA, $CD45RA^+CCR7^-$), and naive subsets (N, $CD45RA^+CCR7^+$). cTfh cells were predominately CM and EM cells (Figure 4A). The memory distribution differed between cTfh subsets, with Th1-cTfh cells being dominated by EM cells, and Th2-cTfh and Th17-cTfh cells being dominated by CM cells (Figures 4B and 4C). For all Tfh subsets, there was a decrease in CM and an increase in EM memory phenotypes after infection (Figure 4D). The differing distribution of memory phenotypes between cTfh subsets in malaria-naive adults is in contrast to the reported memory phenotypes of cTfh cells in Malian children, in which both $CXCR3^+$ (Th1-like) and $CXCR3^-$ (Th2/Th17-like) cTfh were ~50% CM cells.[20]

P. falciparum Stimulation of PBMCs from Malaria-Naive Adults Recapitulates Experimental Malaria by Activating All Subsets of cTfh Cells

To further support data showing that experimental malaria infection in adults activates all cTfh cell subsets, we stimulated PBMCs from healthy malaria-naive adults with *P. falciparum* infected and uninfected red blood cells (RBCs) (iRBCs, uRBCs) for 5 days. *In vitro* stimulation of PBMCs from malaria-naive adults has previously been shown to induce $FoxP3^+$ T regulatory cells.[27,28] Consistent with *ex vivo* data of cTfh cells during experimental malaria infection, Th1- and Th2- but not Th17-cTfh cells showed an increase in activation/proliferation markers Ki67, ICOS, and CD38 following *in vitro* stimulation with iRBCs compared to uRBCs. As seen *ex vivo* following experimental infection, Th1-cTfh had higher levels of activation/proliferation than Th2-cTfh (Figure 5). The activation of both Th1- and Th2-cTfh subsets in malaria-naive adult PBMC samples is in contrast to the *in vitro* stimulation of PBMCs from malaria-exposed children, in which activation/proliferation of cTfh is restricted to Th1-cTfh cells.[20]

Isotype-Switched and Functional Antibodies Are Induced following Experimental Malaria Infection

To examine the relationship between cTfh cell activation and the development of protective humoral immunity following experimental *P. falciparum* infection, we analyzed parasite-specific antibodies. We measured antibody responses in all of the participants on days 0, 8, and 14/15, and EOS to intact merozoites, the parasite stage that invades RBCs.[29] Responses peaked at EOS for both IgG and IgM, with a significant increase observed from day 14/15 (Figure S3). We further characterized the antibody response at EOS by assessing IgG subclasses and IgM,[30] along with the magnitude of functional antibodies, which have roles in protective immunity that fixed complement factor C1q[31,32] that is the first step in classical complement activation, bind Fcγ-receptors (FcγR) that are involved in opsonic phagocytosis and antibody-dependent cellular cytotoxicity,[33,34] and mediate opsonic phagocytosis (OPA) by THP-1 monocytes.[35] We measured responses to intact merozoites and to the abundant and immunodominant merozoite antigen and vaccine candidate, MSP2.[36–39] Following infection, IgM and all IgG subclasses specific for merozoites and recombinant MSP2 were increased at EOS (Figures 6A and 6B). The proportion of individuals responding was highest for IgM and IgG1. Similarly, all of the functional antibody responses were significantly increased after infection except for antibody-promoting FcγRIIa binding to merozoites (Figures 6C and 6D). The prevalence of functional antibodies was highest for antibodies that crosslinked FcγRIII to merozoites and MSP2. Functional responses (FcγR binding, C1q fixation, and OPA) were moderately and significantly correlated with IgG1 (r = 0.49–0.76), and less commonly with

Figure 3. Th2-cTfh Are Activated Early in *P. falciparum* Infection

cTfh ($PD1^+CXCR5^+$ CD4) cells were differentiated into subsets based on CXCR3 and CCR6 expression into Th1 ($CXCR3^+CCR6^-$), Th2 ($CXCR3^-CCR6^-$), and Th17-like ($CXCR3^-CCR6^+$) cell subsets.

(A) Subsets as a frequency of cTfh cells after infection.

(B) Activated $ICOS^+$ subsets as a frequency of cTfh cells after infection.

(C) Activated $CD38^+$ subsets as a frequency of cTfh cells after infection.

(D) Activated $ICOS^+$ subsets as a frequency of cTfh cells for each individual study participant following experimental malaria infection. Participants are ranked based on the frequency of $ICOS^+$ cTfh cells before infection. For participants 6,507, 6,505, and 6,506, no sample was available at EOS time point (NA). Flow cytometry-based assays were performed once on whole-blood samples tested in singles.

Data are from 40 individuals at days 0, 8, and 14/15 and 37 individuals at EOS. For (A)–(C), Wilcoxon signed-rank tests compared to day 0 are indicated. Boxplots are Tukey style, with median and IQR. Whiskers are to data point no further than 1.5 × IQR; dots are outlying points. Paired data are joined by lines. Data are from 40 individuals at days 0, 8, and 14/15 and 37 individuals at EOS.

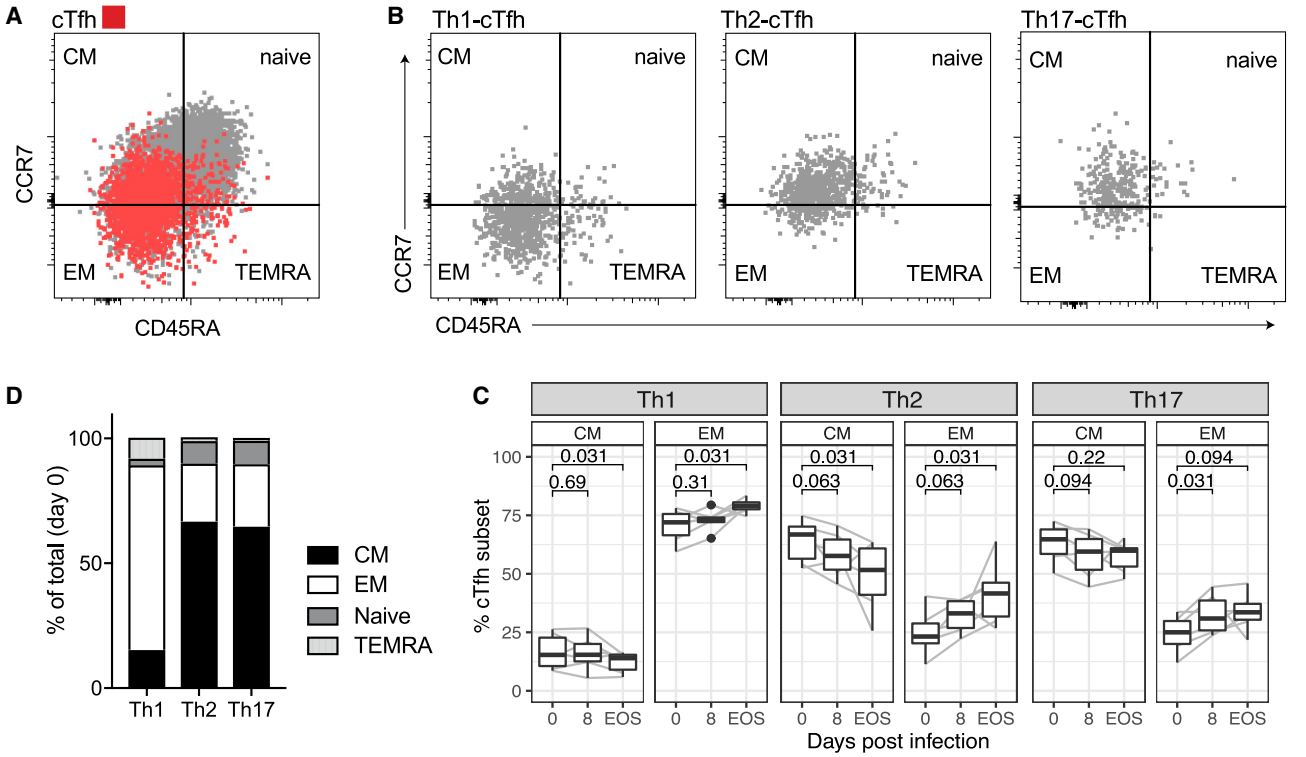

Figure 4. Memory Phenotypes of Tfh Subsets during Infection

(A) cTfh (PD1$^+$CXCR5$^+$CD4) cells were differentiated into memory phenotypes based on CD45RA and CCR7 expression into central memory (CM CD45RA$^-$CCR7$^+$), effector memory (EM CD45RA$^-$CCR7$^-$), terminal differentiated effector memory (TEMRA CD45RA$^+$CCR7$^-$), and naive (CD45RA$^+$CCR7$^+$) phenotypes.

(B) cTfh subsets (Th1, Th2, Th17, based on CXCR3 and CCR6 expression) had different distributions of memory phenotypes.

(C) Mean memory phenotypes across subsets at day 0, before inoculation.

(D) Proportion of CM and EM phenotypes within cTfh subsets after infection. Flow cytometry-based assays were performed once on cryopreserved PBMC samples tested in singles.

Data are from 6 individual study participants from days 0, 8, and EOS (cryopreserved PBMC day 14/15 samples were not available). (A) and (B) are representative data from 1 individual. (C) is the median of each memory phenotype in each subset. (D) Boxplots are Tukey style, with median and IQR. Whiskers are to data point no further than 1.5 × IQR, dots are outlying points. Paired data are joined by lines. Wilcoxon signed-rank test compared to day 0 are indicated.

IgG3 (r = 0.32–0.46). However, each functional response was only moderately correlated to other functions, indicating that functional responses were not equally co-acquired (Figure 6E). IgG1, IgG2, IgG3, and IgM responses but not IgG4 and functional responses were correlated between merozoites and MSP2 (Spearman ρ 0.32–0.68). To understand the overall breadth and composition of an individual's response, each antibody response was categorized as negative (below positive threshold) or low/high (based on below/above median value of all positive responses). The overall composition of induced antibody responses between individuals was diverse; however, there was a clear hierarchy of antibody acquisition (Figure 6F).

Antibody Induction Is Associated with Th2-cTfh Cell Activation during Peak Infection

To calculate a single measure of antibody development to capture the breadth and magnitude of responses across all individuals, regardless of antibody composition, we calculated an antibody score; for each antibody variable (IgG/IgM and functions), responses were scored as 0, 1, and 2 based on their categorized responses of negative/low/high (Figure 6F) and then summed for all merozoite and MSP2 antibodies. The antibody score was normally distributed across the cohort (Figure 7A). To investigate links between cTfh cell activation and antibody score, the change in ICOS$^+$ cTfh cells was calculated for total cTfh between day 0 and subsequent time points and correlated with antibody score. The strongest relationship between antibody score and increase of ICOS$^+$ cTfh cells occurred at day 8 (Figure 7B, frequency change r = 0.3, p = 0.065; Figure S4B, fold change r = 0.31, p = 0.048), suggesting that early activation was most important for antibody induction. This is consistent with an important role for the early activation of cTfh cells in initial phases of GC formation, as previously reported for HIV vaccination in rhesus macaques.[40] To assess the impact of individual subsets at this early day 8 time point, the change in ICOS$^+$ cTfh for each subset was calculated; activation was moderately correlated across subsets (Figure S4A). The positive association between antibody score and ICOS$^+$ cTfh cells at day 8 was restricted to the Th2-cTfh cell subset, suggesting that Th2-cTfh activation is the most important factor in antibody development (Figures 7C and S4C). Neither antibody score nor antibody variables were associated with parasite biomass during infection

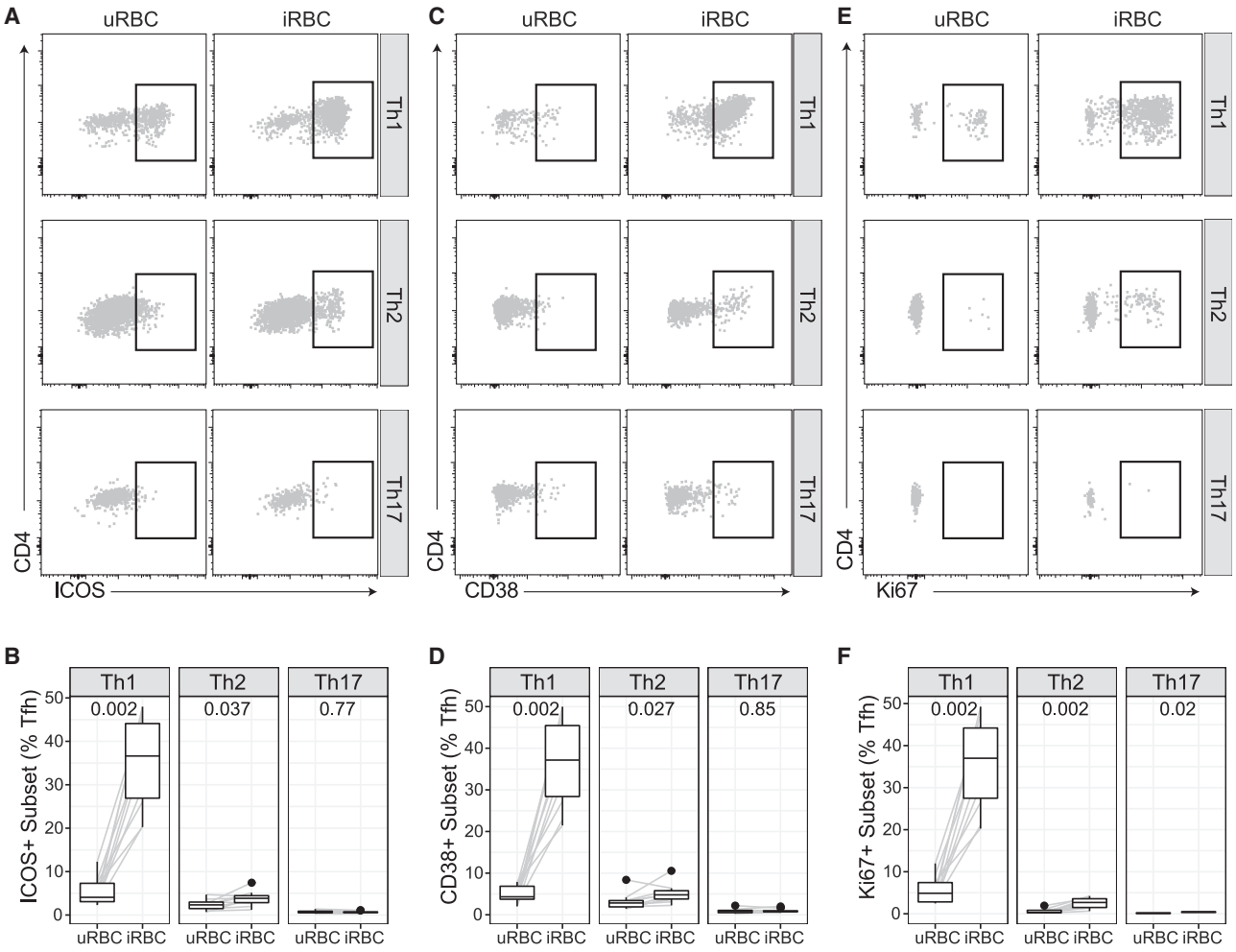

Figure 5. *P. falciparum In Vitro* Stimulation Activates All Subsets of Tfh

PBMCs from malaria-naive healthy donors (n = 10) were stimulated with *P. falciparum*-infected RBCs or uninfected RBCs (iRBCs, uRBCs) for 5 days. Each individual was tested once.

(A and B) ICOS, (C and D) CD38, and (E and F) Ki67 expression on each Tfh subset was compared between uRBC- and iRBC-stimulated cells. (A), (C), and (E) are representative data. (B), (D), and (F) Boxplots are Tukey style, with median and IQR. Whiskers are to data point no further than 1.5 × IQR; dots are outlying points. Paired data are joined by lines. Wilcoxon signed-rank test indicated comparing uRBC to iRBC stimulation in each individual.

(Figures S5A and S5B), in contrast to previous reports.[41–43] Furthermore, antibody induction was not associated with EOS time point nor with infection cohort (Figures S5C–S5E). It has been hypothesized that short-lived plasma cell differentiation may be driven by Th1-cTfh cells.[44] Consistent with this hypothesis, there was a positive association between activated Th1-cTfh cells and total plasma cell expansion at day 14/15 (Figure 7D); we have previously shown that plasma cells are induced at day 14/15 in experimental infections within the same study participants.[45] Plasma cell expansion at day 14/15 was not associated with antibody responses at EOS (r = 0.078, p = 0.63).

DISCUSSION

Despite decades of research, the most advanced malaria vaccine, RTS,S, has only ~30% efficacy in target populations. As antibodies are key mediators of protective human immunity to malaria, it is crucial to understand how antibody responses are induced and maintained. Tfh cells are the key drivers of antibody induction, and optimized activation of Tfh cells during vaccination may boost malaria vaccine efficacy.[6,7] Here, we investigated the role of Tfh activation in antibody responses to malaria infection during experimental *P. falciparum* infection in malaria-naive adults. This experimental human infection model is a powerful system that allows for the longitudinal study of immune responses in previously naive individuals, free of confounding environmental factors commonly seen in malaria-endemic cohort studies. In contrast to Malian children with *P. falciparum* malaria, in whom cTfh cell activation is restricted to Th1 cell subsets,[20] we showed that following experimental infection, the dynamics of cTfh activation are subset specific, with Th2-cTfh cells activated early at peak infection and Th1-cTfh cells activated following treatment. Importantly, we report that the activation of Th2-cTfh cells during peak infection is positively associated with

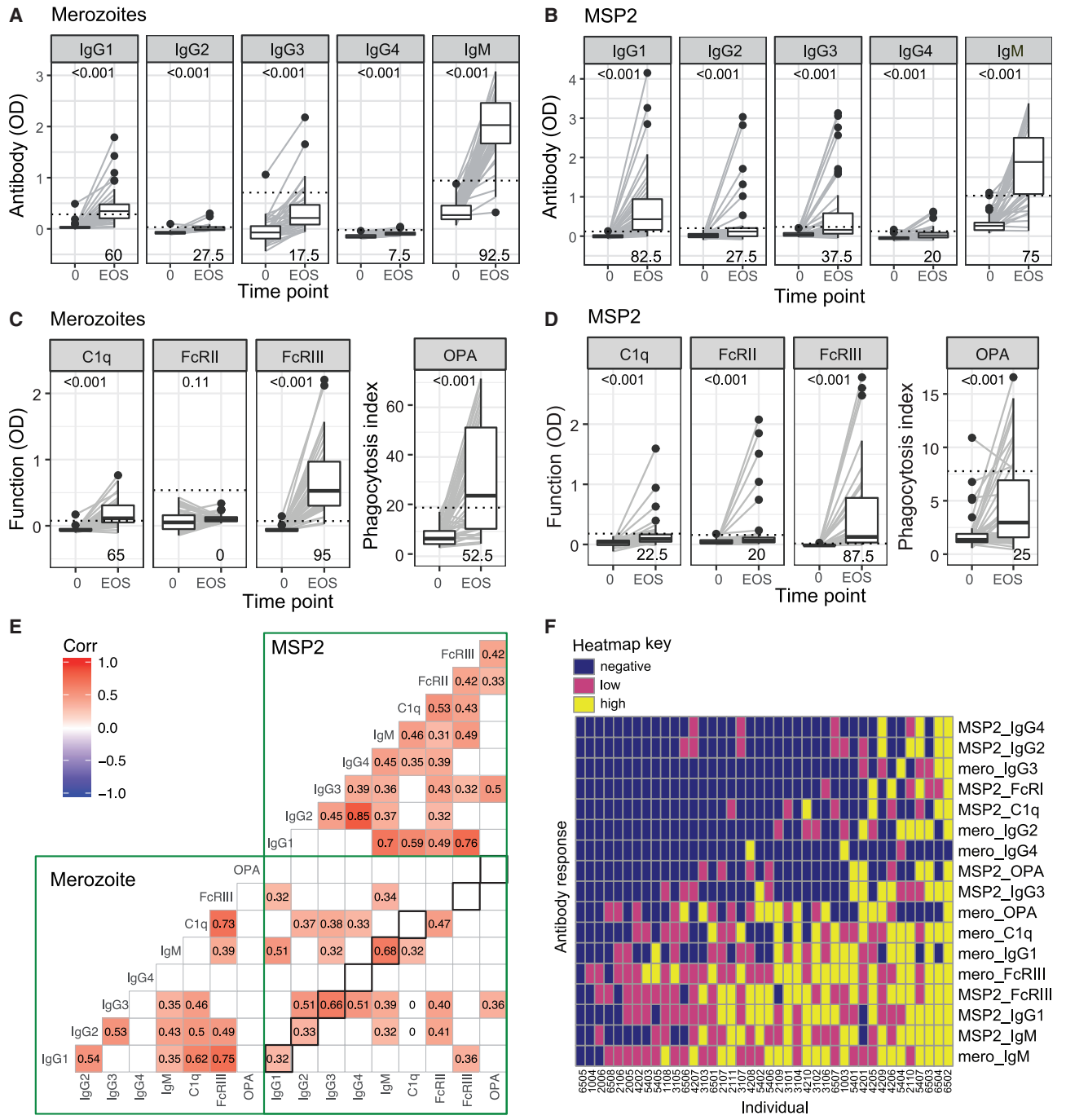

Figure 6. Antibodies to Merozoite and MSP2 Were Induced following IBSM

(A–D) IgG subclasses and IgM responses and functional capacity to fix complement (C1q), bind dimeric FcγRIIa or FcγRIIIa (surrogates for IgG antibody capacity to crosslink cellular receptors), and promote opsonic phagocytosis (OPA) to merozoites (A and C) and MSP2 (B and D) were assessed before inoculation and at EOS time points (n = 40 study participants). The positive threshold for each response is indicated by the dotted line (calculated as mean ± 3 SD of day 0 responses) and the proportion of positive responders are indicated in the bottom right of each panel. The Wilcoxon signed-rank test is <0.001 for all of the comparisons of antibody responses at day 0 to EOS, except for merozoite FcγRIIa, which was not significant (p = 0.11). The phagocytosis index for OPA refers to the percentage of THP-1 monocytes with ingested MSP2 beads. Assays were performed twice independently, with samples tested in duplicates. Boxplots are Tukey style, with median and IQR. Whiskers are to data point no further than 1.5 × IQR; dots are outlying points. Paired data are joined by lines.

(E) Spearman correlation matrix of all antibody responses to merozoites and recombinant MSP2. Only correlations <0.05 are indicated. Correlations between the same subclass/function of responses comparing merozoite and MSP2 responses are indicated by black squares.

(legend continued on next page)

the magnitude and functional breadth of induced anti-malarial antibodies. In contrast, Th1-cTfh cell activation after anti-malaria drug treatment was associated with plasma cell development, which we have previously shown has negative effects on the acquisition of long-lived and memory humoral responses.[45] Thus, we identify contrasting protective and detrimental roles for cTfh cell subset activation during *P. falciparum* malaria.

Understanding the drivers of functional antibody responses will assist in the development of vaccines with the highest protective efficacy. Despite undergoing a relatively low dose of primary infection, our findings show that participants in the clinical trials were able to mount a robust antibody response, including functional antibodies that could fix complement, crosslink FcR, and promote opsonic phagocytosis. Our findings open avenues to identify strategies for generating more potent malaria vaccines. Targeted Tfh cell activation is beginning to be explored as an avenue to improve malaria vaccine efficacy, and antigen-specific cTfh has been identified as one predictor of RTS,S efficacy.[46] Strategies such as using a glycopyranosyl lipid adjuvant/emulsion have been shown to increase the quantity of Tfh cell activation (without changing the composition of the response), resulting in increased magnitude and longevity of induced anti-malarial antibodies in humans.[47] Our results suggest that adjuvants that can also manipulate the composition of Tfh cells to specifically boost Th2-cTfh cell responses may result in further improvements to antibody induction. Precise targeting of Th2-cTfh cells may be necessary; while we cannot formally exclude a positive role of Th1-cTfh in antibody development due to the correlated activation of Tfh subsets, both our results here and previous findings suggest that Th1-cTfh cell activation is not associated with the induction of protective antibodies,[20] but instead disrupts immune acquisition via disruption of GC formation[24,45] and induction of atypical memory B cells.[21] The data presented here suggest that Th1-cTfh may also have a role in disrupting the induction of protective immunity via contributing to the expansion of plasma cells.[45] The majority of blood circulating plasma cells that emerge following vaccination/infection are short lived,[48] and we have shown that during experimental *Plasmodium* infection, these short-lived plasma cells are not involved in the control of parasite replication, but instead act as a nutrient sink that disrupts GC formation and long-lived responses.[45] While we were unable to investigate long-lived responses following experimental infection in humans due to the lack of long follow-up time points of participants, the expansion of plasma cells was not positively associated with antibody induction, consistent with a potential negative role of Th1-cTfh and plasma cell expansion in the acquisition of protective anti-malarial immunity. This finding also may indicate that plasma cells induced during experimental infection may include non-malarial specific responses. Further highlighting the importance of specific Th2-cTfh targeting in vaccine optimization, the co-administration of viral vectored vaccines with RTS,S skewed the cTfh cell response toward Th1-cTfh cell activation, to the detriment of functional antibody induction and vaccine efficacy.[49] In contrast, multiple studies have shown that Th1-Tfh cells are associated with antibody induction to viral infections and vaccinations, including SARS-CoV-2,[16–19] highlighting that distinct vaccine approaches may be required for malaria vaccines compared to viral pathogens.

The association between Th2-cTfh cell activation and antibody acquisition during experimental *P. falciparum* infection is consistent with previously reported properties of Th2-cTfh cells as the cTfh subset with the greatest capacity to activate naive B cells[11] and most similar transcriptionally to GC Tfh cells.[10] Here, we show that Th1- and Th2-Tfh subsets also differ in distribution of memory; Th1-cTfh cells have a predominately central memory phenotype, while Th2-cTfh cells are predominately effector memory cells. After infection, effector memory cells increased in both Th1 and Th2 subsets. Effector memory phenotypes have been reported to indicate bonafide Tfh activity in previous studies.[50] Memory phenotype differences and changes in Tfh subsets may affect the capacity to traffic to and the relative positioning of subsets within lymphoid tissues, and thus involvement of different Tfh subsets in activation of naive and memory B cell populations. In contrast between the positive association between Th2-cTfh and antibody induction, total antigen load was not associated with antibody development, in contrast to previous reported findings.[41–43] These differences between studies may be due to differences in experimental infection models (blood stage versus sporozoite stages) and differences in analytical approaches (including methods to define parasite exposure and antibodies tested). The results seen here indicate that parasite load alone cannot explain antibody development, which is instead governed by individual immune activation, including Th2-cTfh cells. These findings are consistent with our previous reports that suggest that individual intrinsic capacity to respond to infection is important in determining immune responses.[36] Multiple immune factors, including host genetics, age, and prior infections likely contribute to the induction of antibody responses, and future studies are needed to fully understand the factors governing optimal antibody induction during *P. falciparum* infection.

During experimental *P. falciparum* infection, the dynamics of Th2- and Th1-cTfh cell activation appear to be distinct. Th2-cTfh cell activation was detected early at peak infection, while Th1-cTfh cell phenotypic activation was not seen until 1 week after parasite treatment. Clonal analysis of Tfh subsets suggest that Th2- and Th1-cTfh cells are clonally divergent,[8] consistent with distinct development lineages. Little is known regarding the specific induction of Th2-cTfh cells during infection, but transcriptional factor *Ets1* has been reported to be a negative regulator of Th2-Tfh cells.[51] For Th1-Tfh cell activation, preferential induction during *Plasmodium* infection is thought to be mediated by a parasite-driven type I interferon (IFN)-associated IFNγ production.[20,24] We have previously shown that IFNγ production by CD4$^+$ T cells peaks 1 week after treatment in human experimental infection,[52] which is consistent with the peak of Th1-cTfh activation seen here. Whether the switch in cTfh activation profiles from Th2 to Th1 dominance between days 8 and 14/15 is dependent

(F) Heatmap of composition of induced antibodies following categorization as negative (below positive threshold) or low/high (based on below/above median value of all positive responses). Subjects are ranked in order of total breadth and magnitude of response.
See also Figure S3.

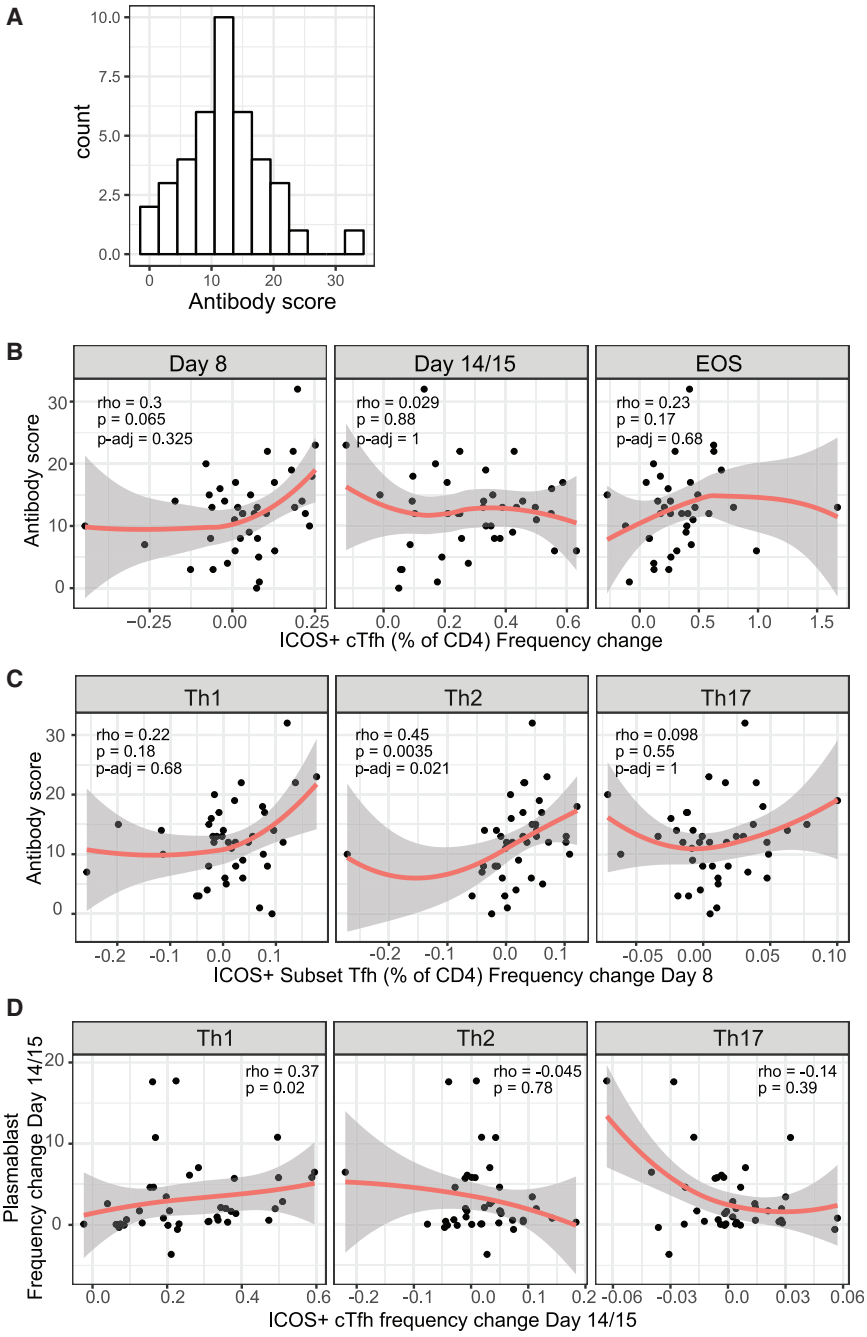

Figure 7. Th2-Tfh Cells Are Associated with Antibody Induction, and Th1-Tfh Cells Are Associated with Plasma Cell Expansion

(A) To assess total breadth and magnitude of antibody response, responses were categorized as negative (0) or low (1) and high (2) responses and combined to calculate a total antibody score.

(B) Association between antibody score and the frequency change of ICOS$^+$ cTfh cells compared to day 0 at each time point.

(C) Association between antibody score and the frequency change of each subset of ICOS$^+$ cTfh cells at day 8.

(D) Association between plasma cell induction and ICOS$^+$ cTfh cells at day 14/15 following infection.

(B–D) Red line is loess. Spearman correlation and ρ are indicated. For (B) and (C), p-adj indicates adjusted p values using the Bonferroni-Holm method for the 6 Tfh comparisons with antibody. See also Figures S4 and S5.

on the treatment or other factors is unknown. It is possible that the Th1-cTfh dominance after treatment occurs because of increased inflammatory responses following parasite death. The distinct dynamics of Th2- and Th1-cTfh cell activation during infection may explain why our longitudinal study with pre-inoculation, peak infection and post-treatment time points detected cell activation in both Th1- and Th2-cTfh subsets, while previous reports in Malian children during a single time point of malaria have observed activation restricted to Th1-cTfh cells.[20] The ability to investigate cTfh activation at specific time points after infection relatively free of other confounders that occur in field studies is a significant strength of our study. However, it is also possible that other factors such as prior exposure, age, or parasite density during infection may play important roles in cTfh cell activation. Shown here in malaria-naive adults, both Th1 and Th2 subsets were activated and proliferated in response to *in vitro* stimulation with *P. falciparum,* in contrast to the restricted activation/proliferation of Th1-Tfh subsets in *P. falciparum*-stimulated PBMCs from Malian children.[20] Further studies are required to identify the factors that control the activation and development of Th2-cTfh cells distinct from Th1-cTfh cells. In addition, further studies are needed to expand our findings to other malaria infection settings and vaccination models.

In conclusion, our findings demonstrate a link between a specific subset of Tfh cells and the induction of robust and functional anti-malarial antibodies. These studies improve our understanding of the dynamics of Tfh cell activation during *P. falciparum* infection in humans and have led to the identification of Th2-cTfh cells as specific Tfh subsets driving anti-malarial antibody production. Due to the central role of functional antibodies in mediating vaccine-induced and naturally acquired protective immunity against malaria, our data have identified Th2-cTfh cells as the key Tfh cell subset that can be targeted to improve anti-malarial vaccine efficacy.

Limitations of Study

Our study uses standard and widely published approaches to identify Th1, Th2, and Th17-cTfh subsets.[10,11,17,20] This strategy

identifies Th2-cTfh as CXCR3^{-}CCR6^{-}, and there is currently no alternative gating strategy to identify Th2-cTfh subsets based on positive marker expression. As such, it is possible that this population contains underappreciated heterogeneity and/or early differentiating cells that may mask the detection of important Tfh subsets involved in antibody induction. Furthermore, we were unable to analyze cellular responses in absolute densities as whole blood counts were not available in our cohorts. Therefore, our results may be confounded by different cell densities across individuals. Moreover, our analysis was limited to peripheral blood samples, and further studies are required to confirm these findings within active germinal centers. While our analysis of functional antibody responses was extensive, we did not make an exhaustive screen of antigen targets and/or functional response; as such, our measure of antibody score is not a true representation of total antibody breadth targeting malaria antigens. We were also unable to analyze antibody and cTfh responses >1 month after malaria inoculation and thus cannot comment on the longevity of induced responses. Furthermore, future studies using more unbiased approaches, such as single-cell RNA sequencing (RNA-seq), and/or more in-depth analysis of Tfh subsets and antibody response, along with longer-term follow-up may reveal better protective Tfh correlates of antibody induction and longevity.

STAR★METHODS

Detailed methods are provided in the online version of this paper and include the following:

- KEY RESOURCES TABLE
- RESOURCE AVAILABILITY
  - Lead Contact
  - Materials Availability
  - Data and Code Availability
- EXPERIMENTAL MODEL AND SUBJECT DETAILS
  - Human studies
  - Plasmodium falciparum *in vitro* culture
- METHOD DETAILS
  - Analytical approaches
  - Calculation of parasite density during infection
  - Flow cytometry
  - *P. falciparum* stimulation of PBMCs from healthy adults
  - Antibodies to merozoites and recombinant MSP2
  - Fcγ receptor-binding assay
  - Coating fluorescent latex beads with antigen
  - Opsonic phagocytosis of antigen-coated beads with monocytes
- QUANTIFICATION AND STATISTICAL ANALYSES

SUPPLEMENTAL INFORMATION

Supplemental Information can be found online at https://doi.org/10.1016/j.xcrm.2020.100157.

ACKNOWLEDGMENTS

RBC and human serum used for parasite culture and naive control sera were provided by the Australian Red Cross Blood Bank (Melbourne). We acknowledge Robin Anders for providing the recombinant MSP2 antigen. We thank the participants involved in the malaria volunteer infection studies, Q-Pharm staff, and Medicine for Malaria Venture for funding the IBSM studies. The graphical abstract was created with BioRender.com. This work was supported by the National Health and Medical Research Council of Australia (program grant 1132975 to J.S.M. and C.R.E.; Practitioner Fellowship 1135955 to J.S.M., Senior Research Fellowship 1154265 to C.R.E., Career Development Award 1141278, Project Grant 1125656, and Ideas Grant 1181932 to M.J.B.; Program Grant 290208, Senior Research Fellowship 1077636 to J.G.B.; Australian Centre for Research Excellence in Malaria Elimination 1134989 to J.G.B. and J.S.M.); and the Jim and Margaret Beever Fellowship to J.-A.C. The Burnet Institute is supported by the NHMRC for Independent Research Institutes Infrastructure Support Scheme and the Victorian State Government Operational Infrastructure Support.

AUTHOR CONTRIBUTIONS

Conceptualization & Methodology, M.J.B., C.R.E., and J.G.B. Investigation & Validation, J.-A.C., F.d.L.R., J.R.L., D.W.A., N.L.D., and A.S.N. (conducted experiments). Formal Analysis, J.-A.C., F.d.L.R., J.R.L., A.S.N., M.J.B., and L.W. Resources, F.H.A., J.S.M., J.G.B., D.W.A., B.D.W., and P.M.H. (provided essential reagents). Supervision, M.J.B., C.R.E., J.G.B., and J.S.M. Writing – Original Draft, Review & Editing, M.J.B., J.-A.C., and C.R.E., with feedback and approval from all of the other authors.

DECLARATION OF INTERESTS

The authors declare no competing interests.

Received: June 17, 2020
Revised: September 8, 2020
Accepted: November 19, 2020
Published: December 22, 2020

REFERENCES

1. World Health Organization (2019). World malaria report 2019. https://www.who.int/publications/i/item/9789241565721.
2. Dobaño, C., Sanz, H., Sorgho, H., Dosoo, D., Mpina, M., Ubillos, I., Aguilar, R., Ford, T., Díez-Padrisa, N., Williams, N.A., et al. (2019). Concentration and avidity of antibodies to different circumsporozoite epitopes correlate with RTS,S/AS01E malaria vaccine efficacy. Nat. Commun. *10*, 2174.
3. White, M.T., Verity, R., Griffin, J.T., Asante, K.P., Owusu-Agyei, S., Greenwood, B., Drakeley, C., Gesase, S., Lusingu, J., Ansong, D., et al. (2015). Immunogenicity of the RTS,S/AS01 malaria vaccine and implications for duration of vaccine efficacy: secondary analysis of data from a phase 3 randomised controlled trial. Lancet Infect. Dis. *15*, 1450–1458.
4. RTS,S Clinical Trials Partnership (2015). Efficacy and safety of RTS,S/AS01 malaria vaccine with or without a booster dose in infants and children in Africa: final results of a phase 3, individually randomised, controlled trial. Lancet *386*, 31–45.
5. Vinuesa, C.G., Linterman, M.A., Yu, D., and MacLennan, I.C. (2016). Follicular Helper T Cells. Annu. Rev. Immunol. *34*, 335–368.
6. Beeson, J.G., Kurtovic, L., Dobaño, C., Opi, D.H., Chan, J.A., Feng, G., Good, M.F., Reiling, L., and Boyle, M.J. (2019). Challenges and strategies for developing efficacious and long-lasting malaria vaccines. Sci. Transl. Med. *11*, eaau1458.
7. Linterman, M.A., and Hill, D.L. (2016). Can follicular helper T cells be targeted to improve vaccine efficacy? F1000Res. *5*, 88.
8. Brenna, E., Davydov, A.N., Ladell, K., McLaren, J.E., Bonaiuti, P., Metsger, M., Ramsden, J.D., Gilbert, S.C., Lambe, T., Price, D.A., et al. (2020). CD4^{+} T Follicular Helper Cells in Human Tonsils and Blood Are Clonally Convergent but Divergent from Non-Tfh CD4^{+} Cells. Cell Rep. *30*, 137–152.e5.
9. Heit, A., Schmitz, F., Gerdts, S., Flach, B., Moore, M.S., Perkins, J.A., Robins, H.S., Aderem, A., Spearman, P., Tomaras, G.D., et al. (2017).

Vaccination establishes clonal relatives of germinal center T cells in the blood of humans. J. Exp. Med. *214*, 2139–2152.

10. Locci, M., Havenar-Daughton, C., Landais, E., Wu, J., Kroenke, M.A., Arlehamn, C.L., Su, L.F., Cubas, R., Davis, M.M., Sette, A., et al.; International AIDS Vaccine Initiative Protocol C Principal Investigators (2013). Human circulating PD-1+CXCR3-CXCR5+ memory Tfh cells are highly functional and correlate with broadly neutralizing HIV antibody responses. Immunity *39*, 758–769.
11. Morita, R., Schmitt, N., Bentebibel, S.-E., Ranganathan, R., Bourdery, L., Zurawski, G., Foucat, E., Dullaers, M., Oh, S., Sabzghabaei, N., et al. (2011). Human blood CXCR5(+)CD4(+) T cells are counterparts of T follicular cells and contain specific subsets that differentially support antibody secretion. Immunity *34*, 108–121.
12. Akiba, H., Takeda, K., Kojima, Y., Usui, Y., Harada, N., Yamazaki, T., Ma, J., Tezuka, K., Yagita, H., and Okumura, K. (2005). The role of ICOS in the CXCR5+ follicular B helper T cell maintenance in vivo. J. Immunol. *175*, 2340–2348.
13. Rasheed, A.U., Rahn, H.P., Sallusto, F., Lipp, M., and Müller, G. (2006). Follicular B helper T cell activity is confined to CXCR5(hi)ICOS(hi) CD4 T cells and is independent of CD57 expression. Eur. J. Immunol. *36*, 1892–1903.
14. Vogelzang, A., McGuire, H.M., Yu, D., Sprent, J., Mackay, C.R., and King, C. (2008). A fundamental role for interleukin-21 in the generation of T follicular helper cells. Immunity *29*, 127–137.
15. Herati, R.S., Muselman, A., Vella, L., Bengsch, B., Parkhouse, K., Del Alcazar, D., Kotzin, J., Doyle, S.A., Tebas, P., Hensley, S.E., et al. (2017). Successive annual influenza vaccination induces a recurrent oligoclonotypic memory response in circulating T follicular helper cells. Sci. Immunol. *2*, eaag2152.
16. Baiyegunhi, O., Ndlovu, B., Ogunshola, F., Ismail, N., Walker, B.D., Ndung'u, T., and Ndhlovu, Z.M. (2018). Frequencies of Circulating Th1-Biased T Follicular Helper Cells in Acute HIV-1 Infection Correlate with the Development of HIV-Specific Antibody Responses and Lower Set Point Viral Load. J. Virol. *92*, 2209.
17. Bentebibel, S.-E., Lopez, S., Obermoser, G., Schmitt, N., Mueller, C., Harrod, C., Flano, E., Mejias, A., Albrecht, R.A., Blankenship, D., et al. (2013). Induction of ICOS+CXCR3+CXCR5+ TH cells correlates with antibody responses to influenza vaccination. Sci. Transl. Med. *5*, 176ra132.
18. Verma, A., Schmidt, B.A., Elizaldi, S.R., Nguyen, N.K., Walter, K.A., Beck, Z., Trinh, H.V., Dinasarapu, A.R., Lakshmanappa, Y.S., Rane, N.N., et al. (2020). Impact of T_h1 CD4 Follicular Helper T Cell Skewing on Antibody Responses to an HIV-1 Vaccine in Rhesus Macaques. J. Virol. *94*, e01737-19.
19. Gong, F., Dai, Y., Zheng, T., Cheng, L., Zhao, D., Wang, H., Liu, M., Pei, H., Jin, T., Yu, D., and Zhou, P. (2020). Peripheral CD4+ T cell subsets and antibody response in COVID-19 convalescent individuals. J. Clin. Invest. Published online November 3, 2020. https://doi.org/10.1172/JCI141054.
20. Obeng-Adjei, N., Portugal, S., Tran, T.M., Yazew, T.B., Skinner, J., Li, S., Jain, A., Felgner, P.L., Doumbo, O.K., Kayentao, K., et al. (2015). Circulating Th1-Cell-type Tfh Cells that Exhibit Impaired B Cell Help Are Preferentially Activated during Acute Malaria in Children. Cell Rep. *13*, 425–439.
21. Obeng-Adjei, N., Portugal, S., Holla, P., Li, S., Sohn, H., Ambegaonkar, A., Skinner, J., Bowyer, G., Doumbo, O.K., Traore, B., et al. (2017). Malaria-induced interferon-γ drives the expansion of Tbethi atypical memory B cells. PLOS Pathog. *13*, e1006576.
22. Portugal, S., Tipton, C.M., Sohn, H., Kone, Y., Wang, J., Li, S., Skinner, J., Virtaneva, K., Sturdevant, D.E., Porcella, S.F., et al. (2015). Malaria-associated atypical memory B cells exhibit markedly reduced B cell receptor signaling and effector function. eLife *4*, e07218.
23. Sullivan, R.T., Kim, C.C., Fontana, M.F., Feeney, M.E., Jagannathan, P., Boyle, M.J., Drakeley, C.J., Ssewanyana, I., Nankya, F., Mayanja-Kizza, H., et al. (2015). FCRL5 Delineates Functionally Impaired Memory B Cells Associated with Plasmodium falciparum Exposure. PLOS Pathog. *11*, e1004894.
24. Ryg-Cornejo, V., Ioannidis, L.J., Ly, A., Chiu, C.Y., Tellier, J., Hill, D.L., Preston, S.P., Pellegrini, M., Yu, D., Nutt, S.L., et al. (2016). Severe Malaria Infections Impair Germinal Center Responses by Inhibiting T Follicular Helper Cell Differentiation. Cell Rep. *14*, 68–81.
25. Hansen, D.S., Obeng-Adjei, N., Ly, A., Ioannidis, L.J., and Crompton, P.D. (2017). Emerging concepts in T follicular helper cell responses to malaria. Int. J. Parasitol. *47*, 105–110.
26. Engwerda, C.R., Minigo, G., Amante, F.H., and McCarthy, J.S. (2012). Experimentally induced blood stage malaria infection as a tool for clinical research. Trends Parasitol. *28*, 515–521.
27. Boyle, M.J., Jagannathan, P., Farrington, L.A., Eccles-James, I., Wamala, S., McIntyre, T.I., Vance, H.M., Bowen, K., Nankya, F., Auma, A., et al. (2015). Decline of FoxP3+ Regulatory CD4 T Cells in Peripheral Blood of Children Heavily Exposed to Malaria. PLOS Pathog. *11*, e1005041.
28. Scholzen, A., Mittag, D., Rogerson, S.J., Cooke, B.M., and Plebanski, M. (2009). Plasmodium falciparum-mediated induction of human CD25Foxp3 CD4 T cells is independent of direct TCR stimulation and requires IL-2, IL-10 and TGFbeta. PLOS Pathog. *5*, e1000543.
29. Boyle, M.J., Wilson, D.W., Richards, J.S., Riglar, D.T., Tetteh, K.K.A., Conway, D.J., Ralph, S.A., Baum, J., and Beeson, J.G. (2010). Isolation of viable Plasmodium falciparum merozoites to define erythrocyte invasion events and advance vaccine and drug development. Proc. Natl. Acad. Sci. USA *107*, 14378–14383.
30. Boyle, M.J., Chan, J.A., Handayuni, I., Reiling, L., Feng, G., Hilton, A., Kurtovic, L., Oyong, D., Piera, K.A., Barber, B.E., et al. (2019). IgM in human immunity to *Plasmodium falciparum* malaria. Sci. Adv. *5*, eaax4489.
31. Boyle, M.J., Reiling, L., Feng, G., Langer, C., Osier, F.H., Aspeling-Jones, H., Cheng, Y.S., Stubbs, J., Tetteh, K.K.A., Conway, D.J., et al. (2015). Human antibodies fix complement to inhibit Plasmodium falciparum invasion of erythrocytes and are associated with protection against malaria. Immunity *42*, 580–590.
32. Reiling, L., Boyle, M.J., White, M.T., Wilson, D.W., Feng, G., Weaver, R., Opi, D.H., Persson, K.E.M., Richards, J.S., Siba, P.M., et al. (2019). Targets of complement-fixing antibodies in protective immunity against malaria in children. Nat. Commun. *10*, 610.
33. Kurtovic, L., Atre, T., Feng, G., Wines, B.D., Chan, J.A., Boyle, M.J., Drew, D.R., Hogarth, P.M., Fowkes, F.J.I., Bergmann-Leitner, E.S., and Beeson, J.G. (2020). Multi-functional antibodies are induced by the RTS,S malaria vaccine and associated with protection in a phase I/IIa trial. J. Infect. Dis. *365*, 1863.
34. Wines, B.D., Vanderven, H.A., Esparon, S.E., Kristensen, A.B., Kent, S.J., and Hogarth, P.M. (2016). Dimeric FcγR Ectodomains as Probes of the Fc Receptor Function of Anti-Influenza Virus IgG. J. Immunol. *197*, 1507–1516.
35. Osier, F.H., Feng, G., Boyle, M.J., Langer, C., Zhou, J., Richards, J.S., McCallum, F.J., Reiling, L., Jaworowski, A., Anders, R.F., et al. (2014). Opsonic phagocytosis of Plasmodium falciparum merozoites: mechanism in human immunity and a correlate of protection against malaria. BMC Med. *12*, 108.
36. Burel, J.G., Apte, S.H., Groves, P.L., Boyle, M.J., Langer, C., Beeson, J.G., McCarthy, J.S., and Doolan, D.L. (2017). Dichotomous miR expression and immune responses following primary blood-stage malaria. JCI Insight *2*, e93434.
37. Feng, G., Boyle, M.J., Cross, N., Chan, J.A., Reiling, L., Osier, F., Stanisic, D.I., Mueller, I., Anders, R.F., McCarthy, J.S., et al. (2018). Human Immunization With a Polymorphic Malaria Vaccine Candidate Induced Antibodies to Conserved Epitopes That Promote Functional Antibodies to Multiple Parasite Strains. J. Infect. Dis. *218*, 35–43.
38. Gilson, P.R., Nebl, T., Vukcevic, D., Moritz, R.L., Sargeant, T., Speed, T.P., Schofield, L., and Crabb, B.S. (2006). Identification and stoichiometry of glycosylphosphatidylinositol-anchored membrane proteins of the human malaria parasite Plasmodium falciparum. Mol. Cell. Proteomics *5*, 1286–1299.

39. McCarthy, J.S., Marjason, J., Elliott, S., Fahey, P., Bang, G., Malkin, E., Tierney, E., Aked-Hurditch, H., Adda, C., Cross, N., et al. (2011). A phase 1 trial of MSP2-C1, a blood-stage malaria vaccine containing 2 isoforms of MSP2 formulated with Montanide® ISA 720. PLOS ONE *6*, e24413.

40. Helmold Hait, S., Vargas-Inchaustegui, D.A., Musich, T., Mohanram, V., Tuero, I., Venzon, D.J., Bear, J., Rosati, M., Vaccari, M., Franchini, G., et al. (2019). Early T Follicular Helper Cell Responses and Germinal Center Reactions Are Associated with Viremia Control in Immunized Rhesus Macaques. J. Virol. *93*, 1241.

41. Biswas, S., Choudhary, P., Elias, S.C., Miura, K., Milne, K.H., de Cassan, S.C., Collins, K.A., Halstead, F.D., Bliss, C.M., Ewer, K.J., et al. (2014). Assessment of humoral immune responses to blood-stage malaria antigens following ChAd63-MVA immunization, controlled human malaria infection and natural exposure. PLOS ONE *9*, e107903.

42. Elias, S.C., Choudhary, P., de Cassan, S.C., Biswas, S., Collins, K.A., Halstead, F.D., Bliss, C.M., Ewer, K.J., Hodgson, S.H., Duncan, C.J., et al. (2014). Analysis of human B-cell responses following ChAd63-MVA MSP1 and AMA1 immunization and controlled malaria infection. Immunology *141*, 628–644.

43. van den Hoogen, L.L., Walk, J., Oulton, T., Reuling, I.J., Reiling, L., Beeson, J.G., Coppel, R.L., Singh, S.K., Draper, S.J., Bousema, T., et al. (2019). Antibody Responses to Antigenic Targets of Recent Exposure Are Associated With Low-Density Parasitemia in Controlled Human *Plasmodium falciparum* Infections. Front. Microbiol. *9*, 3300.

44. Crotty, S. (2019). T Follicular Helper Cell Biology: A Decade of Discovery and Diseases. Immunity *50*, 1132–1148.

45. Vijay, R., Guthmiller, J.J., Sturtz, A.J., Surette, F.A., Rogers, K.J., Sompallae, R.R., Li, F., Pope, R.L., Chan, J.A., de Labastida Rivera, F., et al. (2020). Infection-induced plasmablasts are a nutrient sink that impairs humoral immunity to malaria. Nat. Immunol. *21*, 790–801.

46. Pallikkuth, S., Chaudhury, S., Lu, P., Pan, L., Jongert, E., Wille-Reece, U., and Pahwa, S. (2020). A delayed fractionated dose RTS,S AS01 vaccine regimen mediates protection via improved T follicular helper and B cell responses. eLife *9*, e51889.

47. Hill, D.L., Pierson, W., Bolland, D.J., Mkindi, C., Carr, E.J., Wang, J., Houard, S., Wingett, S.W., Audran, R., Wallin, E.F., et al. (2019). The adjuvant GLA-SE promotes human Tfh cell expansion and emergence of public TCRβ clonotypes. J. Exp. Med. *216*, 1857–1873.

48. Smith, K.G., Hewitson, T.D., Nossal, G.J., and Tarlinton, D.M. (1996). The phenotype and fate of the antibody-forming cells of the splenic foci. Eur. J. Immunol. *26*, 444–448.

49. Bowyer, G., Grobbelaar, A., Rampling, T., Venkatraman, N., Morelle, D., Ballou, R.W., Hill, A.V.S., and Ewer, K.J. (2018). $CXCR3^+$ T Follicular Helper Cells Induced by Co-Administration of RTS,S/AS01B and Viral-Vectored Vaccines Are Associated With Reduced Immunogenicity and Efficacy Against Malaria. Front. Immunol. *9*, 1660.

50. He, J., Tsai, L.M., Leong, Y.A., Hu, X., Ma, C.S., Chevalier, N., Sun, X., Vandenberg, K., Rockman, S., Ding, Y., et al. (2013). Circulating precursor CCR7(lo)PD-1(hi) $CXCR5^+$ $CD4^+$ T cells indicate Tfh cell activity and promote antibody responses upon antigen reexposure. Immunity *39*, 770–781.

51. Kim, C.J., Lee, C.-G., Jung, J.-Y., Ghosh, A., Hasan, S.N., Hwang, S.-M., Kang, H., Lee, C., Kim, G.-C., Rudra, D., et al. (2018). The Transcription Factor Ets1 Suppresses T Follicular Helper Type 2 Cell Differentiation to Halt the Onset of Systemic Lupus Erythematosus. Immunity *49*, 1034–1048.e8.

52. Montes de Oca, M., Kumar, R., Rivera, F.L., Amante, F.H., Sheel, M., Faleiro, R.J., Bunn, P.T., Best, S.E., Beattie, L., Ng, S.S., et al. (2016). Type I Interferons Regulate Immune Responses in Humans with Blood-Stage Plasmodium falciparum Infection. Cell Rep. *17*, 399–412.

53. McCarthy, J.S., Sekuloski, S., Griffin, P.M., Elliott, S., Douglas, N., Peatey, C., Rockett, R., O'Rourke, P., Marquart, L., Hermsen, C., et al. (2011). A pilot randomised trial of induced blood-stage Plasmodium falciparum infections in healthy volunteers for testing efficacy of new antimalarial drugs. PLOS ONE *6*, e21914.

54. Rockett, R.J., Tozer, S.J., Peatey, C., Bialasiewicz, S., Whiley, D.M., Nissen, M.D., Trenholme, K., McCarthy, J.S., and Sloots, T.P. (2011). A real-time, quantitative PCR method using hydrolysis probes for the monitoring of Plasmodium falciparum load in experimentally infected human volunteers. Malar. J. *10*, 48.

55. Gaur, A.H., McCarthy, J.S., Panetta, J.C., Dallas, R.H., Woodford, J., Tang, L., Smith, A.M., Stewart, T.B., Branum, K.C., Freeman, B.B., 3rd., et al. (2020). Safety, tolerability, pharmacokinetics, and antimalarial efficacy of a novel Plasmodium falciparum ATP4 inhibitor SJ733: a first-in-human and induced blood-stage malaria phase 1a/b trial. Lancet Infect. Dis. *20*, 964–975.

56. McCarthy, J.S., Donini, C., Chalon, S., Woodford, J., Marquart, L., Collins, K.A., Rozenberg, F.D., Fidock, D.A., Cherkaoui-Rbati, M.H., Gobeau, N., et al. (2020). A phase 1, placebo controlled, randomised, single ascending dose study and a volunteer infection study to characterize the safety, pharmacokinetics and antimalarial activity of the Plasmodium phosphatidylinositol 4-kinase inhibitor MMV390048. Clin. Infect. Dis. (*April 2*), ciaa368.

57. Collins, K.A., Wang, C.Y., Adams, M., Mitchell, H., Rampton, M., Elliott, S., Reuling, I.J., Bousema, T., Sauerwein, R., Chalon, S., et al. (2018). A controlled human malaria infection model enabling evaluation of transmission-blocking interventions. J. Clin. Invest. *128*, 1551–1562.

STAR★METHODS

KEY RESOURCES TABLE

REAGENT or RESOURCE	SOURCE	IDENTIFIER
Antibodies		
Goat anti-human IgG HRP-conjugate	Thermo Fisher Scientific	Cat#62-8420; RRID:AB_2533962
Mouse anti-human IgG1 subclass (clone HP6069)	Thermo Fisher Scientific	Cat# A-10630; RRID:AB_2534049
Mouse anti-human IgG2 subclass (clone HP6002)	Thermo Fisher Scientific	Cat#05-3500; RRID:AB_2532258
Mouse anti-human IgG3 subclass (clone HP6050)	Thermo Fisher Scientific	Cat#05-3600; RRID:AB_2532261
Mouse anti-human IgG4 subclass (clone HP6025)	Thermo Fisher Scientific	Cat#A10651; RRID:AB_2534053
Mouse anti-human IgM (clone HP6083)	Thermo Fisher Scientific	Cat#054900; RRID:AB_2532927
Goat anti-mouse IgG HRP-conjugate	Merck Millipore	Cat#AP308P; RRID:AB_92635
Goat anti-rabbit IgG HRP-conjugate	Abcam	Cat#AB97051; RRID:AB_10679369
Rabbit anti-human C1q	In-house	Boyle et al.[27]
Strepavidin HRP-conjugate	Thermo Fisher Scientific	Cat#21130
IBSM whole blood panel		
Mouse anti-human CD20 BUV395 (Clone 2H7)	BD Biosciences	Cat#563782; RRID:AB_2744325
Rat anti-human CXCR5 BV421 (Clone RF8B2)	BD Biosciences	Cat#562747; RRID:AB_2737766
Mouse anti-human CD4 V500 (Clone RPA-T4)	BD Biosciences	Cat#560768; RRID:AB_1937323
Mouse anti-human CCR6 BV650 (Clone 11A9)	BD Biosciences	Cat#563922; RRID:AB_2738488
Mouse anti-human CD38 BV786 (Clone HIT2)	BD Biosciences	Cat#563964; RRID:AB_2738515
Mouse anti-human CXCR3 APC (Clone 1C6)	BD Biosciences	Cat#550967; RRID:AB_398481
Mouse anti-human CD27 APC-R700 (Clone M-T271)	BD Biosciences	Cat#565116; RRID:AB_2739074
Mouse anti-human CD8 APC-Cy7 (Clone SK1)	BD Biosciences	Cat#557834; RRID:AB_396892
Mouse anti-human CD19 FITC (Clone HIB19)	BD Biosciences	Cat#55412
Mouse anti-human CD45 PerCP-Cy5.5 (Clone 2D1)	BD Biosciences	Cat#340953; RRID:AB_400194
Mouse anti-human ICOS PE (Clone DX29)	BD Biosciences	Cat#557802; RRID:AB_396878
Mouse anti-human CD3 PE-CF594 (Clone UCHT1)	BD Biosciences	Cat#562280; RRID:AB_11153674
Mouse anti-human PD-1 PE-Cy7 (Clone EH12.1)	BD Biosciences	Cat#561272; RRID:AB_10611585
IBSM PBMC panel		
Mouse anti-human CD45RA BUV563 (Clone HI100)	BD Biosciences	Cat#612926; RRID:AB_2870211
Mouse anti-human CD4 BUV737 (Clone OKT4)	BD Biosciences	Cat#612748; RRID:AB_2870079
Rat anti-human CXCR5 BV421 (Clone RF8B2)	BD Biosciences	Cat#562747; RRID:AB_2737766

(*Continued on next page*)

Continued

REAGENT or RESOURCE	SOURCE	IDENTIFIER
Mouse anti-human CCR6 BV650 (Clone 11A9)	BD Biosciences	Cat#563922; RRID:AB_2738488
Mouse anti-human PD-1 APC(Clone EH12.1)	Biolegend	Cat#329908; RRID:AB_940475
Mouse anti-human CD3 FITC (Clone UCHT1)	BD Biosciences	Cat#555332; RRID:AB_395739
Mouse anti-human CCR7 PerCP-Cy5.5 (Clone 150503)	BD Biosciences	Cat#561144; RRID:AB_10562553
Mouse anti-human CXCR3 PE-CF594 (Clone 1C6)	BD Biosciences	Cat#562451; RRID:AB_11153118
Mouse anti-human Ki67 BUV395 (B56)	BD Biosciences	Cat#564071; RRID:AB_2738577
Mouse anti-human HLA-DR APC-H7 (G46-6)	BD Biosciences	Cat#561358; RRID:AB_10611876
Live Dead Zombie Aqua	Biolegend	Cat#423102
In vitro pRBC stim panel- control PBMC		
Mouse anti-human CXCR3 Pacific Blue (Clone G025H7)	Biolegend	Cat#353724; RRID:AB_2561442
Mouse anti-human CXCR5 BV711 (Clone 12G5)	Biolegend	Cat#356934; RRID:AB_2629526
Mouse anti-human CCR6 BV650 (Clone 11A9)	BD Biosciences	Cat#563922; RRID:AB_2738488
Mouse anti-human CD3 AF532 (Clone UHCT1)	Invitrogen	Cat#58003842
Mouse anti-human CD4 PerCP-Cy5.5 (Clone OKT4)	Biolegend	Cat#317428; RRID:AB_1186122
Mouse anti-human PD-1 PE-Cy7 (Clone EH12.1)	BD Biosciences	Cat#561272; RRID:AB_10611585
Hamster anti-human ICOS APC-Cy7 (Clone C398.4A)	Biolegend	Cat#313530; RRID:AB_2566128
Mouse anti-human Ki67 FITC (Clone B56)	BD Biosciences	Cat#584071
Mouse anti-human CD38 BV480 (Clone HIT2)	BD Biosciences	Cat#566137; RRID:AB_2739535
Live Dead Zombie NIR	Biolegend	Cat#423106
Biological Samples		
Human serum samples	QIMR-Berghofer	McCarthy et al.[39]
Human PBMCs	QIMR-Berghofer	McCarthy et al.[39]
Chemicals, Peptides, and Recombinant Proteins		
Merozoite Surface Protein 2 (MSP2)	HEK293 Freestyle cells	McCarthy et al.[39]
FcγR binding - rsFcγRIIa H131 ectodomain dimer	HEK293 Freestyle cells	Wines et al.[34]
FcγR binding - rsFcγRIIIa V158 ectodomain dimer	HEK293 Freestyle cells	Wines et al.[34]
Purified complement C1q	Merck Millipore	Cat#204876
Experimental Models: Organisms/Strains		
Humans inoculated with *P. falciparum* 3D7-parasitised erythrocytes	QIMR-Berghofer	McCarthy et al.[39]
Software and Algorithms		
R Studio	Version 1.1.456	https://rstudio.com/
GraphPad Prism	Version 7	https://www.graphpad.com/scientific-software/prism/
Flowjo	Version 10.6	https://www.flowjo.com/

RESOURCE AVAILABILITY

Lead Contact

Further information and requests for resources and reagents should be directed to and will be fulfilled by the Lead Contact, Michelle Boyle (Michelle.Boyle@qimrberghofer.edu.au).

Materials Availability

This study did not generate new unique reagents.

Data and Code Availability

This study did not generate any unique datasets or code.

EXPERIMENTAL MODEL AND SUBJECT DETAILS

Human studies

Induced Blood Stage Malaria (IBSM) inoculum preparation, volunteer recruitment, infection, monitoring and treatment were performed as previously described.[53] In brief, healthy malaria naive individuals underwent IBSM inoculation with 2800 viable *P. falciparum* 3D7-parasitized RBCs, and peripheral parasitemia was measured at least daily by qPCR as described previously.[54] Participants were treated with antimalarial drugs at day 8 of infection when parasitemia reaches approximately 20,000 parasites/ml. Blood samples from 40 volunteers (from 4 studies across 6 independent cohorts) were collected prior to infection (day 0), at peak infection (day 8) and 14 or 15 and 27-36 days (end of study, EOS) after inoculation (in analyses these time points are grouped as 0, 8, 14/15 and EOS). Plasma was collected from lithium heparin whole-blood samples according to standard procedures, snap frozen in dry ice and stored at −70°C. In some cohorts, PBMCs were isolated by Ficoll-Paque (Sigma, USA) density gradient centrifugation, isolated PBMCs were cryopreserved in 10% DMSO/FBS. Participants were healthy malaria naive adults (n = 40 (90% male), age 25.5 [21.25-31], median[IQR]) with no prior exposure to malaria or residence in malaria-endemic regions. Clinical trials were registered at ClinicalTrials.gov NCT02867059,[55] NCT02783833,[56] NCT02431637,[57] NCT02431650.[57] For trials NCT02867059,[55] NCT02783833,[56] NCT02431637[57] all participants received the same study drug (no-randomization). For NCT02431650,[57] participants were randomized 1:1 to receive study drug or control. Samples used here was from opportunistic sampling from volunteers who consented to donate blood for immunological studies within the parent clinical trial. As such, no sample size estimation was performed for this immunology study. All consenting individuals were used for Tfh and antibody analysis. 40 individuals were available at day 0, 8 and 14/15. 37 individuals were available at EOS. PBMCs from healthy non-infected controls was collected by the same processes for *P. falciparum in vitro* stimulation for Figure 5 n = 10 (50% female), age 40 [33-55] median[IQR]).

Written informed consent was obtained from all participants. Ethics approval for the use of human samples in the relevant studies was obtained from the Alfred Human Research and Ethics Committee for the Burnet Institute (#225/19), and from the Human Research and Ethics Committee of the QIMR-Berghofer Institute of Medical Research Institute (P1479, P3444 and P3445). Ethical approval for the clinical trials from which the IBSM study samples were collected was likewise gained from the Ethics Committee of the QIMR-Berghofer Medical Research Institute.

Plasmodium falciparum *in vitro* culture

P. falciparum 3D7 parasites were maintained in continuous culture in RPMI-HEPES medium supplemented with hypoxanthine (370 μM), gentamicin (30 μg/ml), 25 mM sodium bicarbonate and 0.25% AlbuMAX II (GIBCO) or 5% heat-inactivated human sera in O+ RBCs from malaria-naive donors (Australian Red Cross blood bank).[30] Cultures were incubated at 37°C in 1% O_2, 5% CO_2, 94% N_2 and used for antibody assays. Schizont stage parasites were purified by MACS separation (Miltenyl Biotec), followed by incubation with the protease inhibitor E64 (10 μg/ml) to prevent rupture of the infected erythrocyte membrane. Upon complete development, segmented merozoites were isolated by filtration (1.2 μm), counted by flow cytometry and coated onto ELISA plates for antibody measurements.

Magnet purified infected RBCs (iRBCs) were stored at 1:2 in Glycerolyte 57 Solution (Baxter Healthcare Corporation) for *in vitro* stimulation assays.

METHOD DETAILS

Analytical approaches

Whole blood flow cytometry was done during longitudinal blood collection. Individual samples were stained in singlets. Antibody measures were completed concurrently on all study participants and analyzed in duplicate in two independent assays. Antibody analysis and flow cytometry analysis was done independently and blinded and only linked after completion. Samples for this study were provided through opportunistic sampling of parent drug clinical trials, as such sample-size estimation was not performed. All available samples were included in study and individuals and data was included in analysis.

Calculation of parasite density during infection

Area under the curve (AUC) were calculated using the trapezoidal method on serial $\log_{10}$ transformed parasites/mL data from 4 days p.i. to each of the three defined time points (8, 14/15, and EOS as described previously.[45] Equation 1 below describes the calculation, with t_i being each time point sampled, P_i being the $\log_{10}$ parasites/mL at that time, and T_N being either 8 p.i., 14/15 p.i., or EOS.

$$AUC_{T_N} = \left(\sum_{t_i=4}^{t_{i+1}=T_N} \frac{(P_i + P_{i+1}) \times (t_{i+1} - t_i)}{2} \right), \quad \text{(Equation 1)}$$

Samples where parasitemia was not detected were substituted with 0 on the $\log_{10}$ scale. The samples collected between the 4 defined time points (ranging from daily to twice daily before treatment, ranging from daily to every two hours after treatment, and ranging from every four days to daily between time point 14/15 and EOS) were used in the calculation of AUC but not in any other analyses.

Flow cytometry

Briefly, 200 μL of whole blood or thawed PBMCs (n = 6) were stained with antibodies using standard protocols. For whole blood, samples were stained with surface antibodies (Key Resources Table) and RBCs were lysed with FACS lysing solution (BD) and re-suspended in 2% FBS/PBS. PBMCs were stained with surface antibodies (Key Resources Table) and were washed with 2% FBS/PBS. All samples were acquired on the BD LSRFortessa™ 5 laser cytometer (BD Biosciences). These data were analyzed using FlowJo version 10.6 software (Tree Star, San Carlos, CA, USA) and all antibodies were purchased from BD Biosciences or Bio-Legend. All samples were included in analysis.

P. falciparum stimulation of PBMCs from healthy adults

In vitro activation of Tfh subsets was assessed in 1 million PBMCs stimulated with parasite-infected RBCs (iRBCs) or uninfected RBCs (uRBCs) (prepared as described in the previous section). PBMCs isolated from malaria naive donors were stimulated for 5 days at a ratio of 1:3 (PBMC: iRBC/uRBC), in culture media (10% FBS/ RPMI-HEPES) at 37°C, 5% CO_2. After 5 days, cells were stained with surface antibodies (Key Resources Table) to identify Tfh subset activation. Stained PBMCs were washed with 2% FBS/PBS, permeabilized (Fix Perm, Ebioscience) and stained with intracellular Ki-67 (B56). Data were acquired on an Aurora 3 (Cytek Biosciences, USA).

Antibodies to merozoites and recombinant MSP2

The level of antibody isotypes targeting merozoites were measured by standard ELISA methods as previously described.[30] Briefly, 96-well flat bottom MaxiSorp® plates (Nunc) were coated with 50 μl of *P. falciparum* 3D7 merozoites (2.5 X 10^5 merozoites/ml) or 50 μl of 0.5 μg/ml MSP2 recombinant antigen[53] in PBS overnight at 4°C. Plates were blocked with 150μl of 10% skim milk in PBS for merozoites or 1% casein in PBS (Sigma-Aldrich) for MSP2 for 2 hours at 37°C. Human serum samples were diluted in 0.1% casein in PBS and incubated for 2 hours at room temperature. For total antigen specific IgG detection, plates were incubated with goat polyclonal anti-human IgG HRP- conjugate (1/1000; Thermo Fisher Scientific) for 1 hour at room temperature. For detection of IgG subclasses and IgM, plates were incubated with a mouse anti-human IgG1 (clone HP6069), mouse anti-human IgG3 (HP6050) or mouse anti-human IgM (clone HP6083) at 1/1000 (Thermo Fisher Scientific) for 1 hour at room temperature. This was followed by detection with a goat polyclonal anti-mouse IgG HRP-conjugate (1/1000; Millipore). For all ELISAs, plates were washed three times with PBS-Tween 0.05% between antibody incubation steps. For ELISA plates coated with isolated merozoites, washes were performed with PBS without Tween to prevent parasite lysis. Serum dilution used for merozoites was 1/100 for IgG, 1/250 for IgG subclasses and IgM, 1/100 for C1q and FcγR. Serum dilution used for MSP2 was 1/100 for IgG, 1/250 for IgG subclasses and IgM, 1/100 for C1q and 1/50 for FcγR. For detection of complement fixing antibodies, following incubation with human sera, plates were incubated with purified C1q (10 μg/ml; Millipore) as a complement source, for 30 min at room temperature. C1q fixation was detected with rabbit anti-C1q antibodies (1/2000; in-house) and a goat anti-rabbit-HRP (1/2500; Millipore). TMB liquid substrate (Life Technologies) was added for 1 hour at room temperature and the reaction was stopped using 1M sulfuric acid. The optical density (OD) was read at 450 nm. Standardization of the assays was achieved using positive control plasma pools on each plate. Background values (wells with no plasma) were subtracted from all values of other wells, and positivity was determined as the mean plus 3 standard deviations of the OD from naive plasma samples at day 0 prior to inoculation. Assays were performed twice independently with samples tested in duplicates. To investigate the relationship between antibody responses and Tfh cells, antibody responses below positive cut-off threshold were set as negative, and remaining positive responses were used to calculate median and used to categorise responses into low (below median) and high (above median) responses. Antibody score was calculated by giving categories zero/low/high a numerical score of 0/1/2 and then summing across all antibody responses. Calculation of antibody score was preformed independently of Tfh analysis. All samples were included in analysis.

Fcγ receptor-binding assay

A standard ELISA protocol was modified to measure the level of antibody-mediated FcγR binding.[33,34] 100 μL of recombinant protein at 0.5 μg/ml was coated on Maxisorp plates (Nunc) and incubated overnight at 4°C, followed by 3 washes with PBS-Tween 0.05%.

The plates were then blocked with 200 μL of 1% BSA in PBS (PBS-BSA) at 37°C for 2 hours followed by 3 washes with PBS-Tween 0.05%. Serum samples were diluted at 1:100 in PBS-BSA and 100 μL of each sample was added to the ELISA plates in duplicate and incubated at room temperature for 2 hours, followed by 3 washes in PBS-Tween. 100ul of biotin-conjugated rsFcγRIIa H131 or rsFcγRIIIa V158 ectodomain dimer (0.2ug/ml) was added to each well and incubated at 37°C for 1 hour followed by 3 washes with PBS-Tween. This was followed by a secondary horseradish peroxidase (HRP)-conjugated streptavidin antibody (1:10,000) in PBS-BSA at 37°C for 1 hour followed by 3 washes with PBS-Tween 0.05%. Finally, 50 μL of TMB liquid substrate was added for 20 minutes to measure enzymatic reactivity. The reaction was stopped with 50 μL of 1M sulfuric acid solution. The level of binding was measured as optical density at 450 nm. Pooled human IgG from malaria-exposed adults (1/100) and rabbit was used as positive controls. Individual sera from naive Melbourne adults (1/100) were used as negative controls. Assays were performed twice independently with samples tested in duplicates.

Coating fluorescent latex beads with antigen

Amine-modified fluorescent latex beads (Sigma) were washed twice with 400 μL of PBS and centrifuged at 3000 g for 3 min.[33] 400 μL of 8% glutaraldehyde (diluted in PBS) was added to the beads and incubated on a roller overnight at 4°C. After washing with PBS, 1mg/ml of recombinant MSP2 was added to the mixture and incubated while vortexing for 4 hours. Following this, the mixture was centrifuged, and the pellet was collected as the bound protein fraction. 200ul of ethanolamine was added to the pellet to quench amine groups and incubated for 30 min while vortexing. The pellet was subsequently washed in PBS and blocked with 1% BSA overnight at 4°C. The antigen-coated beads were stored 4°C in the presence of 0.1% SDS and 0.02% sodium azide.

Opsonic phagocytosis of antigen-coated beads with monocytes

The density of latex beads coated with recombinant MSP2 was adjusted to $5x10^7$ beads/ml and opsonised with serum samples (1/10 dilution) for 1 hour.[33,37] Samples were washed 3 times with RPMI-1640 before co-incubation with THP-1 monocytes for phagocytosis. Phagocytosis was allowed to occur for 20 min at 37°C and samples were subsequently washed with FACS buffer at 300 g for 4 minutes. The proportion of THP-1 cells containing fluorescent-positive beads was evaluated by flow cytometry (FACS CantoII, BD Biosciences), analyzed using FlowJo software and presented as phagocytosis index (the percentage of THP-1 monocytes with ingested MSP2 beads).

QUANTIFICATION AND STATISTICAL ANALYSES

Data analysis was performed in RStudio 1.1.456 or GraphPad Prism 7. Non-parametric analysis was performed for all comparisons and assumptions of normality were not performed. Paired data of immune responses between time points was analyzed by Wilcoxon signed rank test. Correlations between responses were analyzed by Spearman's correlation. Statistical details including the statistical tests used, the exact value of n (representing the number of samples tested), definition of center and dispersion/precision measures can be found in the figure legends. Statistical significance is defined as the conventional significance level of less than 0.05.

Cell Reports Medicine, Volume *1*

Supplemental Information

Th2-like T Follicular Helper Cells Promote Functional Antibody Production during *Plasmodium falciparum* Infection

Jo-Anne Chan, Jessica R. Loughland, Fabian de Labastida Rivera, Arya SheelaNair, Dean W. Andrew, Nicholas L. Dooley, Bruce D. Wines, Fiona H. Amante, Lachlan Webb, P. Mark Hogarth, James S. McCarthy, James G. Beeson, Christian R. Engwerda, and Michelle J. Boyle

Supplementary Figure S1

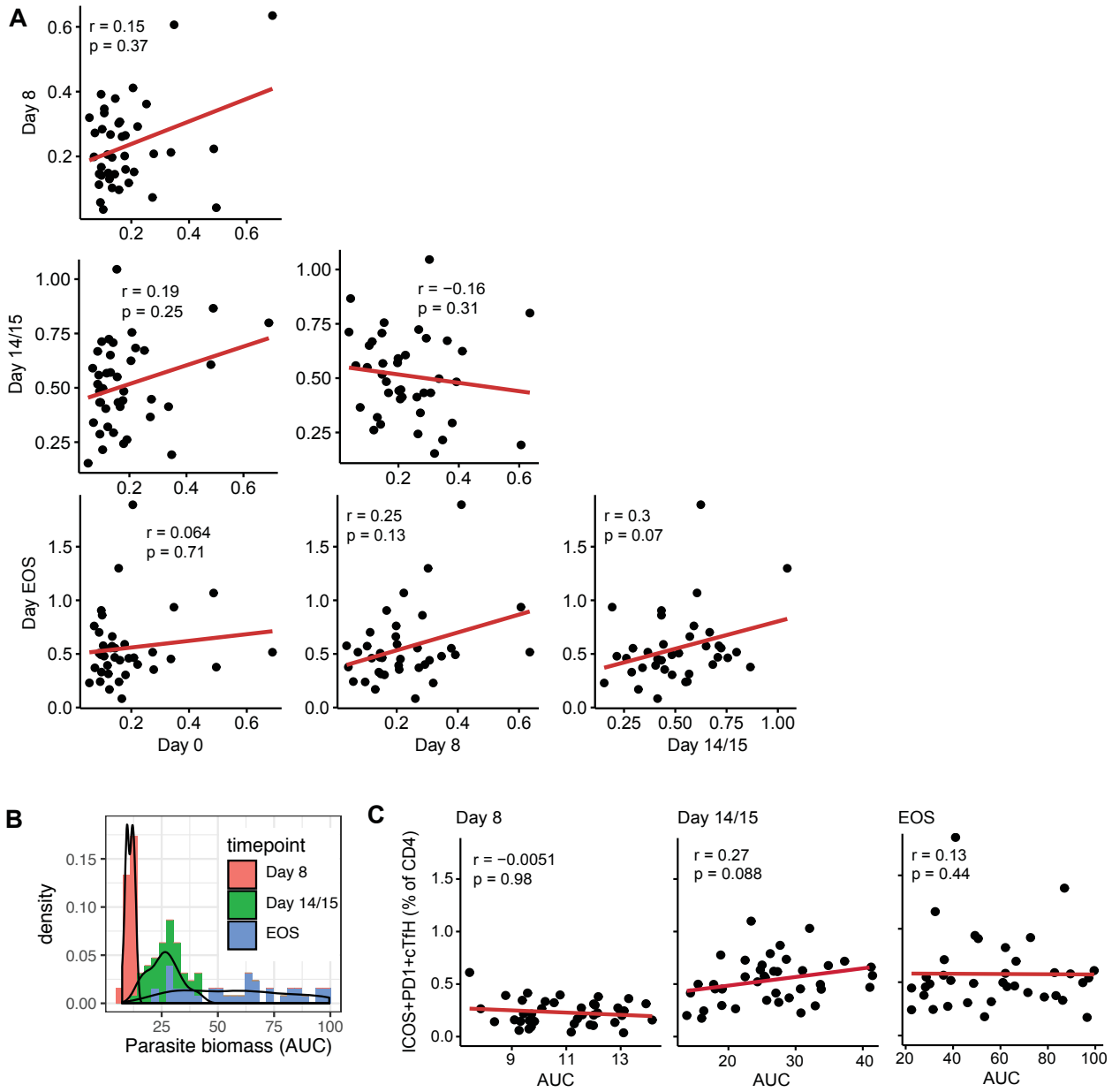

Supplementary Figure S1 Correlations between ICOS+ cTfh cells and parasite biomass

A) Correlations between ICOS+ cTfh (PD1+CXCR5+, data is % of CD4 T cells) at each time point (day 0, 8, 14/15 and end-of-study). Spearman's correlations coefficients and *p* values indicated. **B)** Parasite biomass was calculated as Area Under the growth Curve (AUC) on the $\log_{10}$ scale from inoculation to day 8 (day of treatment), day 14/15 and end-of-study time points from qPCR data. **C)** Correlations between ICOS+ cTfh and parasite density (area under curve, AUC) at each time point.

Related to Figure 2 in the main manuscript.

Supplementary Figure S2

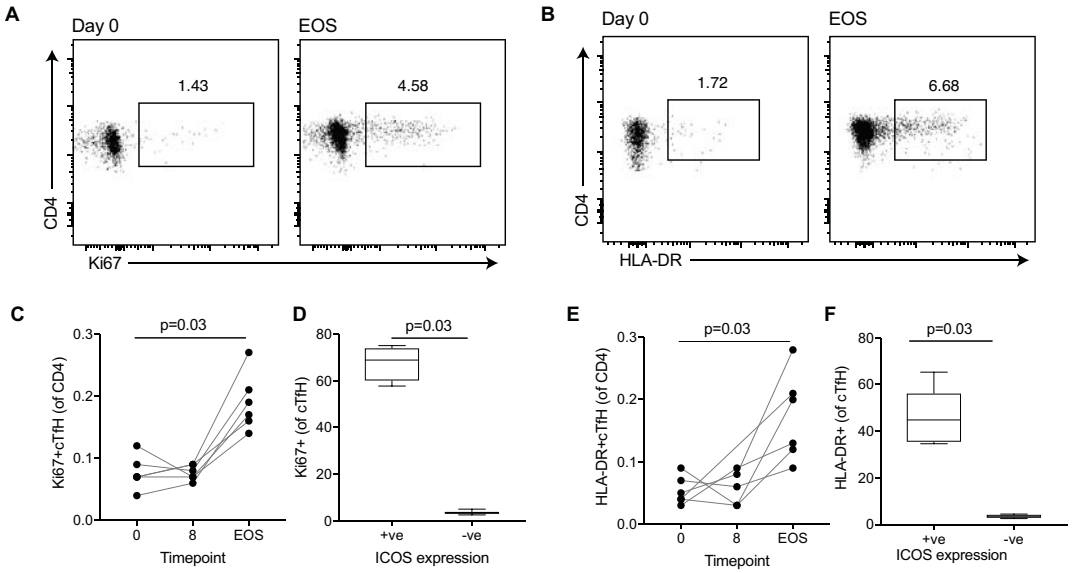

Supplementary Figure S2: Ki67 and HLA-DR expression on cTfh

PBMC samples from a subset of 6 participants were assessed for Ki67 **(A)** and HLA-DR **(B)** expression on cTfh (PD1+CXCR5+) at days 0, 8 and EOS time-points. The frequencies of Ki67+ **(C)** and HLA-DR+ **(E)** PD1+cTfh increased during experimental infection. Expression of Ki67 and HLA-DR was higher on ICOS+ than ICOS- cTfh subsets **(D**, **F)**. Wilcoxon signed rank test indicated.

Related to Figure 3 in the main manuscript.

Supplementary Figure 3

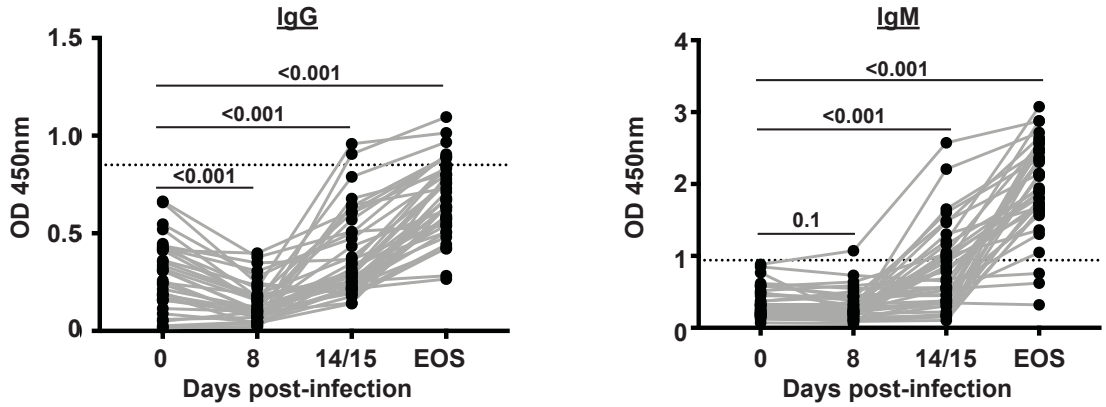

Supplementary Figure S3: Antibody responses to intact 3D7 merozoites increased following experimental infection

Total IgG and IgM levels were measured to intact 3D7 merozoites at all timepoints. Antibody levels are expressed as optical density (OD) values measured at 450nm; dotted line represents the antibody positive threshold calculated as mean + 3SD of day 0 responses; *p* values were calculated using a Wilcoxon signed rank test.

Related to Figure 6 in the main manuscript.

Supplementary Figure S4

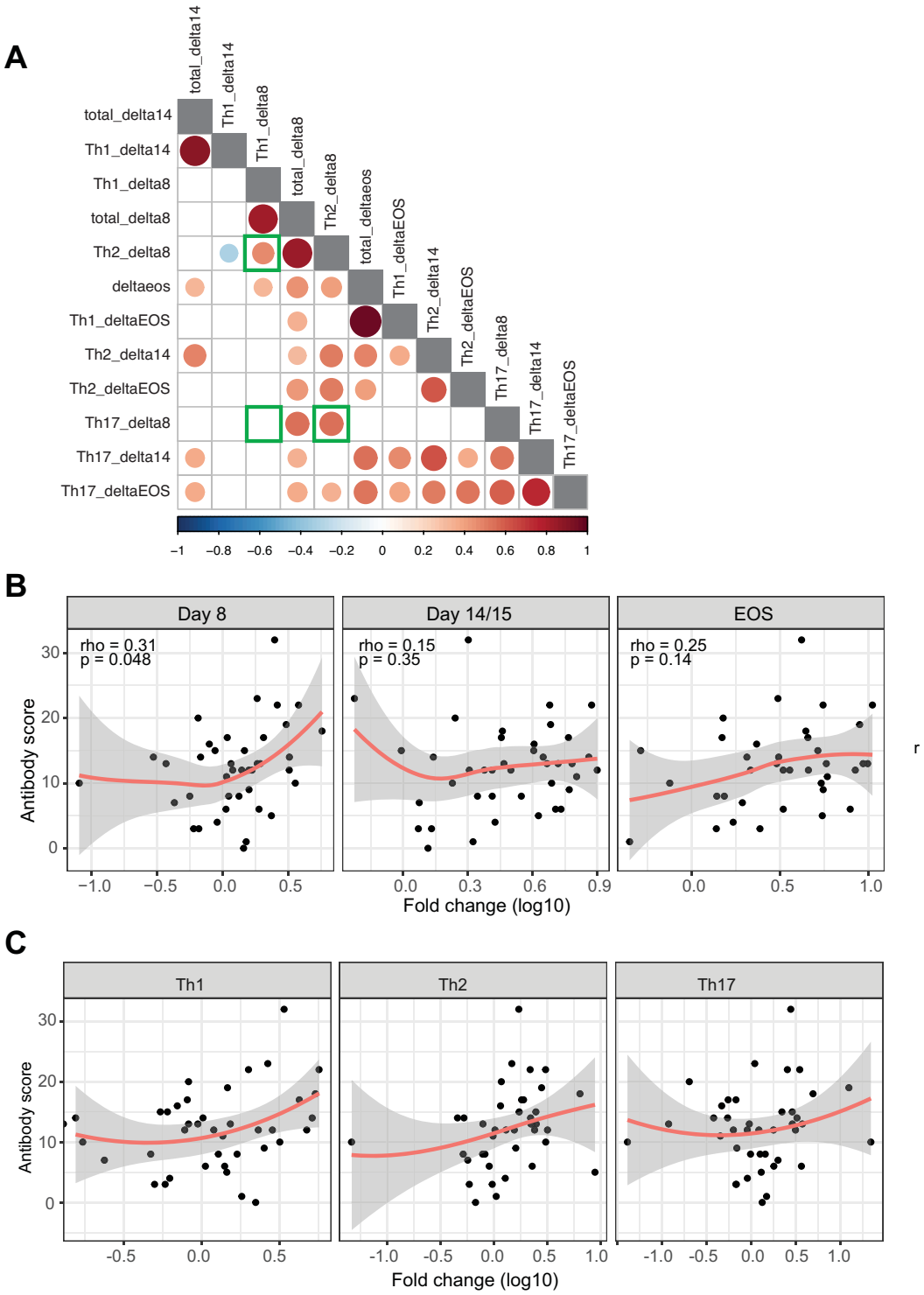

Supplementary Figure S4: Association between antibody score and fold change in cTfh activation

A) Correlation between antibody score and the fold change of total ICOS+ cTfh at day 8, day 14/15 and EOS. **B)** Correlation between antibody score and fold change of ICOS+ cTfh subsets at day 8 following experimental infection. **C)** Correlation between antibody score and fold change of ICOS+ cTfh subsets at day 8 following experimental infection.

Related to Figure 7 in the main manuscript.

Supplementary Figure S5

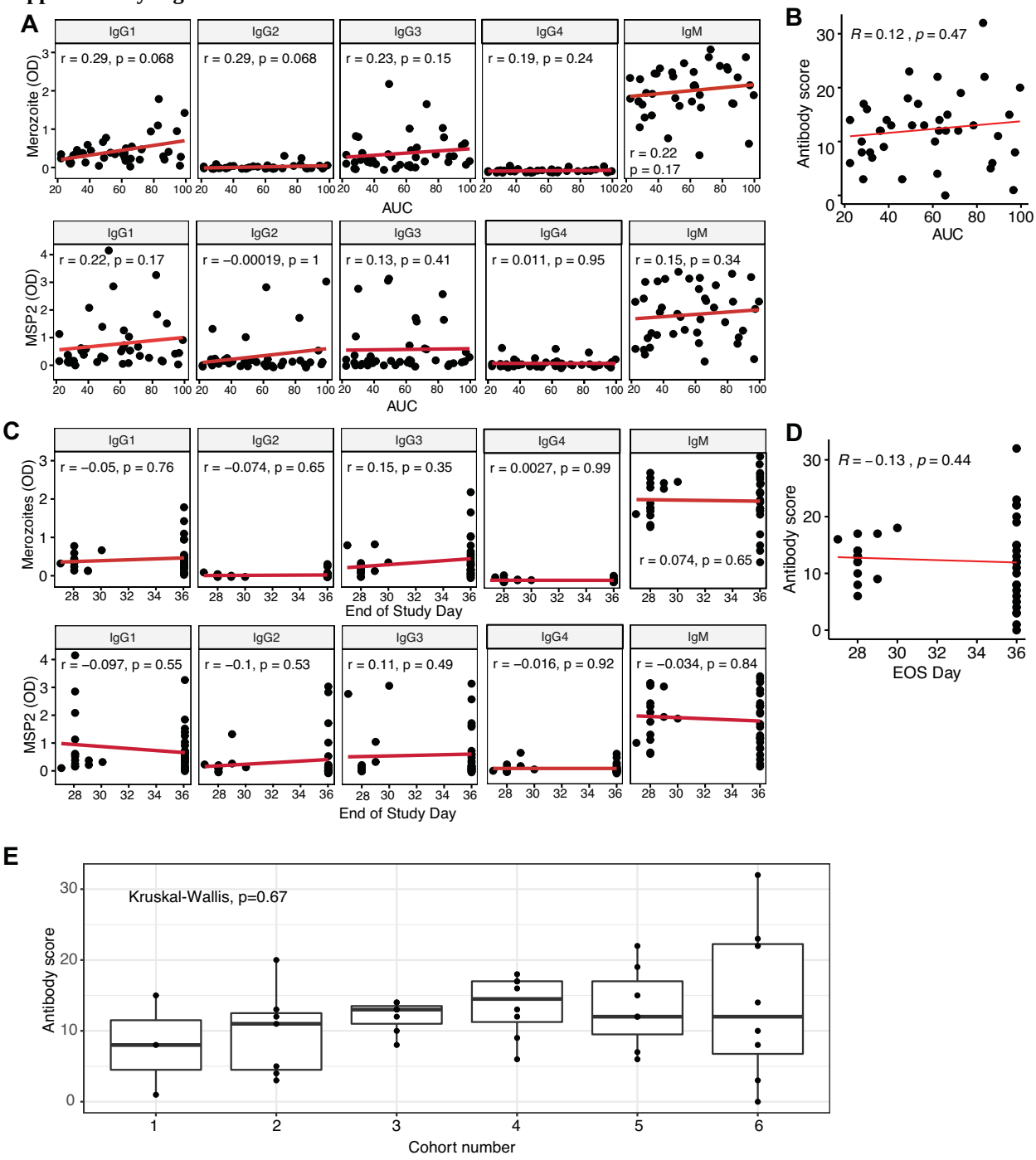

Supplementary Figure S5 Relationship between antibodies and parasite burden

A) Correlation between individual antibody responses to merozoites and MSP2 with parasite biomass as measured by area under curve at EOS time point. **B)** Correlation between total antibody score with parasite biomass at EOS time point. **C)** Correlation between individual antibody responses to merozoites and MSP2 and EOS day. **D)** Correlation between total antibody score and EOS day. Correlations were evaluated using Spearman's rho. **E)** Antibody score in each infection cohort. Kruskal-Wallis indicated.

Related to Figure 7 in the main manuscript.